THE INFLUENCE OF ORTHODONTIC APPLIANCES ON MAGNETIC RESONANCE IMAGING OF THE VELOPHARYNX

by

Eshan Pua Schleif

December, 2022

Director of Dissertation: Dr. Jamie L. Perry, PhD

Major Department: Communication Sciences and Disorders

Magnetic resonance imaging (MRI) is becoming increasingly valuable among cleft palate craniofacial teams in patients with velopharyngeal insufficiency (VPI). One hindrance to the growing use of MRI among the cleft population is the presence of orthodontic appliances, which could result in image distortions and non-interpretability of MR images. This is particularly a challenge because individuals with cleft anatomy have a higher incidence of dental anomalies compared to the non-cleft population. Dental anomalies are present in approximately 62% of patients with isolated cleft lip and 96.7% of patients with both cleft lip and palate. Previous MRI studies of the brain revealed that some appliances and dental materials cause image distortions which result in non-interpretability of MR images, while others do not interfere with visibility of desired structures. Currently, it is not known which orthodontic appliances and materials hinder visualization of the velopharyngeal structures during an MRI. The purpose of this study is to evaluate the influence of common pediatric orthodontic appliances on VP MRI. Insights from this study will be useful in determining which patients undergoing orthodontic treatment are candidates for VP MRI.

This study included nineteen participants undergoing orthodontic treatment. All participants were scanned in a 1.5-Tesla Siemens MRI machine in supine position, capturing 3D and 2D images at rest and during sustained phonation. Two of the commonly used MR

sequences for the evaluation of the VP were compared. Two raters experienced in performing MRI evaluations of the velopharynx examined the MRI for distortion in 8 anatomical sites of interest.

The results of this study demonstrate that some appliances such as hyrax palatal expanders and braces with stainless steel brackets are recommended for a VP MRI, while class II corrector springs are not recommended. The HASTE MRI sequence with 2D imaging techniques should be utilized, while FSE and 3D imaging techniques are not recommended. VP MRI of participants with orthodontic appliances is recommended for clinical cases when information about the LVP muscle length, LVP origin distance, and/or distance from velar knee to posterior pharyngeal wall needs to be obtained. Other forms of imaging, such as lateral cephalogram, should be utilized for this population to determine hard palate length, velar length, pharyngeal depth, and effective velar length. The presence of wire spring coils and molar bands are likely to not to interfere with the MRI evaluation.

Findings from this study suggest that the presence of orthodontic appliances does not hinder visualization of all velopharyngeal structures during an MRI. Therefore, careful consideration must be made prior to disqualifying or recommending patients for VP MRI. The results of this study will be useful in determining which patients undergoing orthodontic treatment are candidates for VP MRI.

The Influence of Orthodontic Appliances on Magnetic Resonance Imaging of the Velopharynx

A Dissertation

Presented to the Faculty of the Department of Communication Sciences and Disorders

East Carolina University

In Partial Fulfillment of the Requirements for the Degree

Doctor of Philosophy in Rehabilitation Sciences

By

Eshan Pua Schleif

December, 2022

Director of Dissertation: Jamie L. Perry, PhD
Dissertation Committee Members:
Xiang Ming Fang, PhD
Patrick M. Briley, PhD

DEDICATION

I dedicate this dissertation to God Almighty, my Creator, the Giver of life, who is the reason I have breath and life. He called me to this doctoral program, and it was by His grace that I was able to complete this degree. To Jesus, the Son of God, Christ my Savior, who died so that I may have life and life eternal. To Holy Spirit, who was my Helper in every step of the process, who gave encouragement when I wanted to give up. To God be the glory forever and ever!

ACKNOWLEDGMENTS

First and foremost, I would like to thank my mentor, Dr. Jamie Perry, who was the first to see potential in me and invited me to be her graduate research assistant before she even met me. She believed in me and took a risk to take me under her wing. If not for her support, I would not have completed a master's thesis project which then led me to pursue a PhD. I am thankful for the hours she spent on the phone with me, reviewing my writing, counseling me, sharing her past experiences and wisdom with me. She was patient with my mistakes and reasonable with her expectations. She was supportive every step of the way, even helping me walk through how to balance life as a new mother while balancing the PhD workload. Thank you for always reminding me that I am a good writer and never giving up on me.

My sincere thanks to the other members of my dissertation committee: Dr. Xiangming Fang and Dr. Patrick Briley. Their guidance, support, and valuable feedback during every stage of this study were incredible. I am very appreciative of their time, and especially their willingness to meet in person to discuss research design, statistical approaches, and interpretation of findings. I have spent extended time with each of them for other projects, and they were always collaborative and supportive of my work.

I am thankful for Dr. Van Wallace McCarlie, who provided insightful feedback and was critical in the success of this project. His expertise in orthodontics and research methods was a huge asset. Amid his busy schedule, he made time to help with patient recruitment at his clinic. Without his help and support, I could not have completed this project.

I would also like to thank the faculty members at my alma mater Butler University who first inspired me to love the field of speech language pathology and helped me develop as a student, researcher, and clinician. Dr. Suzanne Reading, Dr. Carolyn Richie, Dr. Mary Gospel,

Mrs. Ann Bilodeau have all been amazing professors who have greatly contributed to my professional and personal development.

A huge thanks to Dr. John Riski from Children's Healthcare of Atlanta who was my supervisor during my clinical fellowship year at the Center for Craniofacial Disorders. He was an inspiration to me in the way he integrated research with clinical practice. He emphasized the importance of clinical and doctoral training. Without his example, I would never have pursued this degree.

Thank you to one of my greatest colleagues, Neda Tahmasebifard. Neda and I began this journey at the same time, and I could not have made it through the program without her. I will always remember our deep conversations in and outside of lab, the conferences we roomed together at and attended together, and the many presentations we rehearsed for one another. Neda reminded me that I am not alone in this journey and supported me through the most vulnerable times. I am proud of Neda's accomplishments and thankful for her friendship.

I am thankful for my loving father and mother, who were huge supporters in my pursuit of a PhD. As a young child, I witnessed my father's hard work and long hours he poured into completing his doctoral program. His strength and determination are always an inspiration and constant encouragement to me. I am also thankful for the countless hours my mom spent on her knees in prayer over me.

Last but not least, I would like to thank my amazing husband, Samuel Schleif, who has been my co-laborer in this program. He was my biggest cheerleader, my greatest supporter. He believed in me when I didn't believe in myself. He spoke encouragement to me in the hardest times. I am thankful for the many hours he cared for our son, so I can complete the work I needed to do for my PhD. I consider this degree as much his as it is mine.

TABLE OF CONTENTS

LIST OF TABLES

LIST OF FIGURES

Chapter 1: Literature Review

Facial Growth

Facial growth seldom occurs in a balanced and equal manner, but instead, in varying directions and unequal amounts (Lande, 1952; Inouye, 1957; Subtelny, 1959; Bjork, 1963). However, a harmony of growth amount, direction, and degree of rotation is required between the maxilla and mandible to achieve normal facial proportions (Lavergne & Gasson, 1976; Lavergne & Gasson, 1978; Isaacson, Isaacson, Speidel, & Worms; 1971; Isaacson, Zapfel, Worms, Bevis, & Speidel, 1977; Isaacson, Zapfel, Worms, & Erdman, 1977; Hultgren, Isaacson, Erdman, Worms, & Rekow, 1980; Isaacson, Erdman, & Hultgren, 1981; Schudy, 1963; Schudy, 1964; Schudy, 1965). There are several ways to describe the relationship between the maxilla and mandible. A misalignment or incorrect relationship between the maxilla and mandible is described as a malocclusion. The Angle's classification was introduced over a century ago and is accepted as the gold standard of classifying malocclusions in dental practice (Angle, 1899). A Class I malocclusion molar relationship is when the mesiobuccal cusp of the maxillary first molar occludes with the mesiobuccal groove of the mandibular first molar. Class II malocclusion is when the mesiobuccal groove of the mandibular first molar is posteriorly positioned when in occlusion with the mesiobuccal cusp of the maxillary first molar. Class III malocclusion is when the mesiobuccal cusp of the maxillary first molar occludes posteriorly to the mesiobuccal groove of the mandibular first molar.

The use of cephalometric radiography is another commonly used method for describing the alignment between the maxilla and mandible (Rakosi, 1982). As shown by figure 1.1, four anatomical landmarks including the midpoint of the sella turcica (S), nasion or the most anterior point of the fronto-nasal suture (N), the point of deepest concavity anteriorly on the maxillary alveolus (A), and the point of deepest concavity anteriorly on the mandibular symphysis (B). The

SNA angle represents the relative anteroposterior position of the maxilla to the cranial base and is the angle formed by the SN line and the NA line. The SNB angle represents the relative anteroposterior position of the mandible to the cranial base and is the angle formed by the SN line and the NB line. When the SNA or SNB angle is higher than the average value, it indicates that the jaw is positioned more anteriorly than the typical individual. When the SNA or SNB angle is lower than the average value, it indicates that the jaw is positioned more posteriorly than the typical individual (Mitchell et al., 2013; Whaites & Drage, 2013; Heasman, 2009; British Standards Institute, 1983). Average values reported by Steiner's and Delaire's cephalometric analyses are commonly used for preoperative planning of orthognathic surgery (Delaire, 1971; Delaire, 1978; Delaire, Schendel, & Tulasne, 1981; Steiner, 1953; Steiner, 1959; Steiner, 1960). The ANB angle represents the relative anteroposterior position of the maxilla to the mandible and is the angle formed by the NA line and the NB line. The ANB angle can be used to determine skeletal class. An ANB angle between 2-4 degrees is classified as a Class I malocclusion. If the ANB angle is less than 2 degrees, it is classified as a Class III malocclusion and if it is greater than 4 degrees, it is classified as a Class II malocclusion.

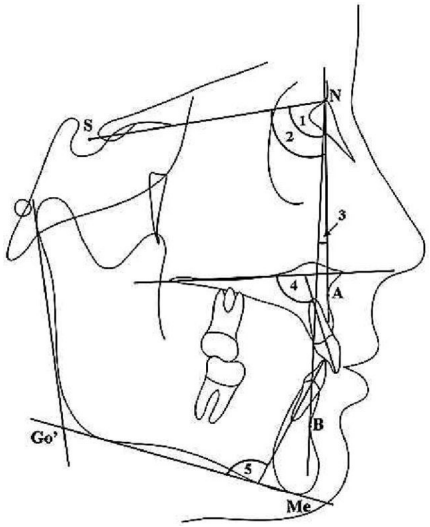

Figure 1.1 Cephalometric measurements published by Chaimanee, Suzuki, & Suzuki (2011)

Between ages 3 and 22 years, facial growth is greatest in the anteroposterior direction (depth), less in the vertical dimension (height), and least in the transverse dimension (width) (Hellman, 1933). Beginning from age 7, little change in maxillary prognathism is observed, but rather an increase in SNB angle due to the proportionally greater increase in mandibular prognathism (Bjork, 1951; Lande, 1952).

The direction and degree of mandibular rotation is correlated with the direction and degree of condylar growth (Bjork, 1963; Odegaard, 1970). As the condyles grow in the vertical direction, the mandible rotates in a forward, bite-closing direction (Bjork, 1963). Simultaneously, the degree of mandibular rotation is balanced with the amount of maxillary growth to maintain adequate vertical and anteroposterior relationships (Lavergne & Gasson, 1978; Schudy, 1964). For example, extreme vertical or forward (bite-closing) rotation of the maxilla requires a compensatory amount of mandibular rotation and condylar growth. Therefore, growth of the maxilla often plays a leading role in the amount and direction of facial development (Lande, 1952, Schudy, 1964; Schudy, 1965; Creekmore, 1967).

Facial growth and development of occlusion are also closely related (Hellman, 1933; Bjork, 1951). Changes in molar position have been shown to be characteristic of different types of facial rotation (Bjork & Skieller, 1972). Maxillary molar eruption typically occurs when vertical midface development has slowed (Sinclair & Little, 1985). In response to the amount of mandibular growth at the condyle, mandibular molars will display mesial tipping with upward and forward movement of the mandibular incisors (Bjork & Skieller, 1972). The concept of "dental compensation" has been described in response to skeletal changes to maintain the integrity of the occlusion. In normal occlusion, there is increase in auriculonasion dimension (from external auditory meatus to nasion in the sagittal plane) and concomitant forward

adjustment of the entire face (Hellman, 1933). When the second molars begin to erupt, there is more backward growth in the jaw region and slight forward maxillary adjustment. Once eruption of second molars have completed, there is no more forward adjustment, but considerable backward growth.

The growth and adjustment in faces with class III malocclusion is different, specifically in the measurements of facial depth (Hellman, 1933). There is an increase in auriculonasion dimension, less in the auriculo-prosthion (from external auditory meatus to prosthion) and infradentale (between mandibular central incisors at gum line), but more in the goniomenton (from gonion/mandibular angle to menton). Adjustment occurs chiefly in the mandible and in forward direction. Since the maxilla is involved in guiding the development of the dentofacial complex, cessation or inhibition of vertical maxillary growth leads to greater anterior component of mandibular growth (Creekmore, 1967).

A significant amount of sexual dimorphism has been described regarding the nature and extent of facial changes seen post-puberty (Sinclair & Little, 1985). Males demonstrate a significant amount of late condylar growth and growth continues until an older age compared to females. This results in a greater degree of late mandibular rotation and increase in mandibular prognathism, and larger facial proportions in males. In response, maxillary growth may not be complete until 15 years of age in females (Bjork, 1966; Bjork & Skieller, 1977) and 18 years of age in males (Savara & Singh, 1968; Broadbent et al., 1975).

Class III Malocclusion and Midface Hypoplasia

For individuals with class III malocclusion, the position of the mandibular molars is anterior to maxillary molars, leading to problems with breathing, mastication, and speech.

Approximately 7.04% of the general population is affected (Hardy et al., 2012) and 20-40% of individuals with repaired cleft lip and palate (Ross, 1987; Good et al., 2007; Hardy et al., 2012; Saltaji et al., 2012). Individuals with non-cleft anatomy may have maxillary atrophy or obstructive sleep apnea resulting in maxillary hypoplasia. Untreated maxillary hypoplasia can lead to superior rotation of mandible, reduction in facial height, and upward tilt of the occlusal plane. The presence of skeletal imbalance between the maxilla and the mandible often leads to the human body's natural tendency to compensate through adjustment and alterations. The dentition will alter its position in effort to achieve occlusal contact, such as the retroclination of mandibular incisors and proclination of the maxillary incisors. Such compensations of dentition must be addressed with presurgical or postsurgical orthodontic treatment. Many different appliances may be employed to accomplish decompensation of the dentition including palatal expanders, headgear, braces, and interarch elastics (Wirthlin & Shetye, 2013).

LeFort I osteotomy is the most common surgical method for correction of malocclusion, as it allows for movement of the maxilla in all three planes (Iannetti et al., 2004; Buchanan & Hyman, 2013). In severe cases of class III malocclusion or patients with obstructive sleep apnea, a bimaxillary (two-jaw) or bilateral sagittal split osteotomy (BSSO) may be considered (Smatt & Ferri, 2005). LeFort I with BSSO is where both maxilla and mandible osteotomies are completed (Buchanan & Hyman, 2013). Bimaxillary operation can increase volume of the oro- and nasopharyngeal airway if obstruction is at the skeletal level (Smatt & Ferri, 2005). Bimaxillary operation may be needed to compensate the degree of maxillary advancement with mandibular setback (Johnston et al., 2006).

LeFort I Osteotomy History and Technique

LeFort I osteotomy is named after the fracture pattern extending from the nasal septum through the pterygomaxillary junction, originally described by Rene LeFort in 1901 (Buchanan & Hyman, 2013). It was first used for correction of dentofacial deformities in 1921 by Herman Wassmund, who implemented this method to reposition the maxilla (Wassmund, 1927). The technique is now widely published and used in collaboration with orthodontic treatment for correction of dentofacial abnormalities (Converse & Horowitz, 1969).

This procedure requires local anesthesia injected into the gingivobuccal sulcus of the upper lip with the patient lying in supine position with neutral head position. Nasotracheal intubation is often preferred for occlusal checks during the procedure. The first incision is made through the mucosa and into loose areolar tissue in the submucosal plane to expose the maxilla. After the maxilla is exposed, a reciprocating saw is used to make medial and lateral osteotomies are made according to the plans made to meet the aesthetic needs of the patient. The same osteotomy is performed on the contralateral side. Lastly, curved osteotomies are used to separate the pterygomaxillary junction.

Once osteotomies are completed, downfracturing of the maxilla is performed which allows for further dissection of the nasal floor and nasal mucosa. Once the maxilla is free, the soft tissue is stretched for increased range of motion and mobilized using forceps or with digital pressure. The maxilla is then repositioned according to preoperative treatment plans. Bone grafts from facial bones, iliac crest, or the cranium may be considered to provide more stable movement if large gaps are created for large movements. Maxillomandibular fixation (MMF) may be used while the maxilla is repositioned and fixed in place with titanium plates and screws. After proper occlusion is ensured, the incision is closed with absorbable sutures. Postoperatively,

a nasogastric tube is kept for 24 hours, and the patient is discharged after he/she is tolerating liquids and pain is managed. A soft mechanical diet is recommended 4-6 weeks following the procedure to ensure proper bone union (Buchanan & Hyman, 2013).

Relapse

Relapse occurs in approximately 10-20% of patients with non-cleft anatomy and 19-50% of patients with cleft anatomy (Thongdee & Samman, 2005; Cheung et al., 2006; Scolozzi, 2008; Chua et al., 2010; Saltaji et al.,2012; de Haan et al., 2013; Yamaguchi et al., 2016; Dowling et al., 2005; Proffit et al., 1987; Bell et al., 1977; Bishara et al., 1988). The maxilla tends to relapse backward with counterclockwise rotation and the mandible tends to relapse forward with clockwise rotation, both tending toward an anterior open bite, opposing the correction. Relapse occurs mostly in the first 6 months following the procedure but could continue to persist up to 1 year post-operatively (Willmar, 1975; Posnick & Ewing, 1990; Eskenazi & Schendel, 1992; Dowling et al., 2005). Varying results in rate of relapse may be due to corrections in multiple planes simultaneously (Buchanan & Hyman, 2013). Clinically significant relapse is described as relapse greater than 2mm (Dowling et al., 2005; Proffit et al., 1996; Bell et al., 1977; Bishara et al., 1988). Studies report little to no difference between the rates of relapse in single jaw versus bimaxillary surgery, likely because the degree of mean maxillary advancement was similar in both groups (Carlotti & Schendel, 1987; Iannetti et al., 1987; Posnick & Ewing, 1990; Fahradyan et al., 2018).

Some studies report a positive relationship between amount of maxillary advancement and horizontal relapse (Fahradyan et al., 2018; Houston et al., 1989; Hochban et al., 1993; Kiely et al., 2006; Hirano & Suzuki, 2001; Dowling et al., 2005). Other studies report no association

between the two (Proffit et al., 1987; Posnick & Ewing, 1990; Louis et al., 1993; Watts et al., 2015; Bhatia et al., 2016), demonstrating maxillary stability even after 10-22mm of anteroposterior movement (Bhatia et al., 2016). Several studies note that bone grafting of maxillary osteotomy sites had a protective effect on relapse, resulting in an average of 1.723mm less relapse compared to patients without bone grafting (Gomes et al., 2013; Eser et al., 2015; Fahradyan et al., 2018).

Patients with repaired cleft palate consistently present with higher rates of relapse (Hochban et al., 1993; Chua, Hägg, & Cheung, 2010; Fahradyan et al., 2018; Thongdee & Samman, 2005; Cheung et al., 2006; Chua et al., 2010; Saltaji et al.,2012; de Haan et al., 2013; Yamaguchi et al., 2016). This could be attributed to excessive scar tissue, poor blood supply, more complex maxillomandibular deformity, poor bone quality, and/or deficiency of bone with no significant medial wall of the sinus observed in cleft patients (Ross, 1987; Polley & Figueroa, 1997; Figueroa et al., 2004). Therefore, gradual movement using distraction osteogenesis may often be recommended over traditional LeFort I osteotomy to achieve more stable maxillary position following correction (Chua, Hägg, & Cheung, 2010).

Levator Veli Palatini Muscle and Maxillary Advancement

The levator veli palatini (LVP) is a paired, skeletal muscle and is the most important muscle involved in closure of the velopharyngeal (VP) port (Perry, Kuehn, & Sutton, 2013). The muscle originates at the petrous portion of the temporal bone and courses anteriorly, medially, and inferiorly to insert into the midsection of the velum at approximately 40% of the velar length (Moon & Kuehn, 2004; Perry, 2011a; Boorman & Sommerlad, 1985). The left and right LVP muscle bundles join to create a sling arrangement, visible from the oblique coronal plane of a

magnetic resonance image (MRI). The LVP muscle length can be divided into the extravelar and intravelar segments. The extravelar segment is the distance from the LVP muscle origin at the base of the skull to the midline of the muscle bundle where the muscle inserts into the body of the velum, while the intravelar segment is the distance between the two points of LVP insertion in the body of the velum (Kotlarek et al., 2020). Contraction of the LVP muscle results in superior and posterior movement of the velum from the midportion of the velum, at an approximately 45-degree angle to achieve closure against the posterior pharyngeal wall (Lubker et al., 1970; Bell-Berti, 1976; Kuehn 1979; Perry, 2011a).

During maxillary advancement, anterior movement of the maxilla also results in anterior movement of the hard and soft palate. This advancement has been shown to increase the size of the VP port (McComb et al., 2011) and may result in negative impacts on VP function for speech (Trindade et al., 2003; Impieri et al., 2018; Schultz et al., 2019). It is possible that repositioning of the maxilla may result in alteration of the LVP muscle to a more disadvantageous angle or length, leading to changes in speech (Kuehn et al., 2004; Perry & Kuehn, 2009; Inouye et al., 2015).

Biomechanics of Muscle

Skeletal muscle is composed of thousands of force-producing muscle fibers organized in bundles called fascicles (Ahn et al., 2003; Pappas et al., 2002; Drost et al., 2003). Although the muscle displays parallel-fibered architecture, dynamic magnetic resonance has visualized nonuniform shortening along muscle fascicles (Pappas et al., 2002). This nonuniform shortening is attributed to difference in lengths of the centerline and anterior fascicles and/or the curvature

of the anterior fascicles (Asakawa et al., 2002). This complex fascicle geometry informs passive and active muscle fiber characteristics (Blemker, Pinsky, & Delp, 2005).

The active tensile component incorporates the force-length behavior of skeletal muscle, where peak muscle force is achieved when the muscle is at optimal length and position (Gordon, Huxley, & Julian, 1966). The muscle's optimal length is described as λ_{muscle} =1, where λ_{muscle} is the muscle stretch ratio (λ_{muscle} = 1 is 100% rest position with no contraction and λ_{muscle} = 0.7 is 70% rest position or 30% shortened from rest) (Gordon, Huxley, & Julian, 1966). Increased contraction from a 100% rest position lessens the muscle's force-generating capacity (Inouye et al., 2015; See Figure 1.2). When implementing these properties on the LVP muscle, higher closure force and lower minimum activation required are indicators of better VP function. When closure force is higher, less muscle activation is needed to achieve VP closure, thus resulting in better fatigue avoidance and better muscle endurance.

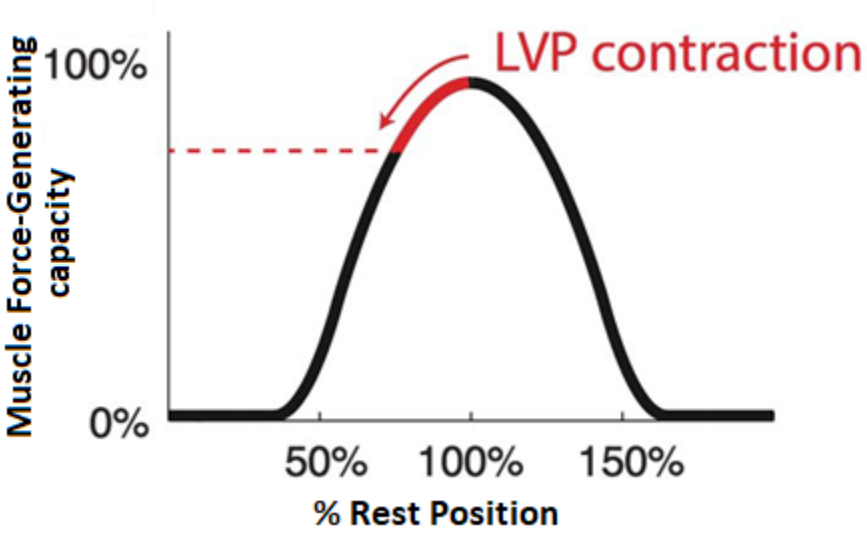

Figure 1.2 Force-length curve of an active muscle describing the relationship between muscle length and force generating capacity, published by Inouye et al. (2015). This curve demonstrates that as contraction increases, muscle force-generating capacity decreases.

Inouye et al. (2015) designed a computational model of the LVP muscle incorporating the passive and active muscle fiber characteristics. Different parameters were adjusted to examine the impact of the adjustments on the VP mechanism. Inouye et al. (2015) reported that the most advantageous anatomy involves a decreased velum-LVP angle, increased velar length, and decreased VP distance compared to the average anatomy. For example, as VP port distance increased, closure force decreased. As extravelar LVP length increased, closure force increased. When the velum-LVP angle increased by rotating the velum anteriorly in the sagittal plane, the closure force decreased. There was a 48% decrease in the muscle activation required when the velum-LVP angle decreased. Authors concluded that the most advantageous anatomies achieved more than twice the closure force of the least advantageous anatomies, demonstrating that some anatomical parameters have much greater influence on VP mechanics compared to others. These findings are particularly important because they suggest that repositioning of the maxilla may result in alteration of the LVP muscle to a more disadvantageous angle, leading to negative impacts on velopharyngeal function.

Findings using Magnetic Resonance Imaging

Advancements in MRI have enabled assessment of the LVP muscle at rest and during speech production using an oblique coronal image plane. Significant findings have been reported in LVP muscle morphology before and after surgery examined using MRI (Perry et al., 2010). Differences in LVP muscle morphology have been observed between individuals with normal VP function and individuals with VP dysfunction (Nakamura et al., 2003; Tian et al., 2010; Kotlarek et al., 2020). Children with velopharyngeal insufficiency (VPI) have been shown to display significantly shorter velar length (Nakamura et al., 2003; Tian et al., 2010), smaller

pharyngeal length-to-depth ratio (Nakamura et al., 2003), larger pharyngeal depth (Tian et al., 2010), and reduced mobility of the velum and lateral pharyngeal walls during phonation (Tian et al., 2010). More recently, Kotlarek et al. (2020) reported larger sagittal angle, smaller effective VP ratio, decreased average extravelar length, and decreased velar thickness at midline in children with cleft anatomy and VPI. Measures such as pharyngeal depth, pharyngeal length-to-depth ratio, sagittal angle, effective VP ratio, and extravelar length may be altered post-operatively for patients undergoing LeFort I osteotomy.

Over the last 20 years, non-sedated MRI for assessment of the velopharynx for children with velopharyngeal insufficiency has been established and routinely used in clinical settings across the country (Kotlarek et al., 2021). A child-friendly protocol with behavioral adaptation and training aspects have been published with reported success rates between 96-100% for children ranging from 4-9 years of age (Tian et al., 2010; Kollara & Perry, 2014; Kollara et al., 2017; Perry et al., 2018; Kollara et al., 2019). Patients considered for surgical management are referred for MRI to provide visualization of velopharyngeal muscles, not visible with other forms of imaging such as nasopharyngoscopy, video fluoroscopy, and lateral radiograph. Imaging outcomes have been reported for numerous surgical procedures common for the cleft population including primary palatoplasty (Perry, 2007); primary palatoplasty with pedicled buccal fat pad flap (Kotlarek et al., 2020; Kotlarek, Perry, & Jaskolka, 2022), primary palatoplasty with buccal flaps (Mann et al., 2020; Haenssler et al., 2021), and sphincter pharyngoplasty (Mason et al., 2021). Investigations examining changes in the velar musculature as a result of maxillary advancement using MRI is limited. This is likely due to the common presence of metal presurgical orthodontic appliances in cleft patients undergoing maxillary advancement which could potentially hinder visualization of the velopharyngeal anatomy (Wirthlin & Shetye, 2013).

Maxillary Advancement and Speech Outcomes

Changes in speech and resonance following maxillary advancement has been reported in cleft and noncleft populations. While the severity of changes leading to VPI is less commonly observed in the noncleft population, several studies have reported changes to resonance following the procedure (Schwarz & Gruner, 1976; Ward et al., 2002; Dalston & Vig, 1984). Schwarz and Gruner (1976) report that articulation in the labio-dental area improved, VP closure deteriorated, and nasal area did not change in all non-cleft patients. Ward et al. (2002) observed altered nasal resonance in 3 of 5 non-cleft patients following LeFort I osteotomy. One of the patients demonstrated worsened hyponasality, and the other two demonstrated onset of hypernasality following the procedure. Dalston and Vig (1984) reported a decrease in nasal resistance and increase in nasal-oral balance following maxillary advancement in 37 of 40 female patients. McCarthy et al. (1979) utilized lateral cephalograms to show expanded nasopharyngeal volume after the procedure. Two studies demonstrated increased angle of the hard and soft palate following maxillary advancement (McCarthy et al., 1979; Schendel et al., 1979). A systematic review by Hassan et al. (2007) examining the effect of orthognathic surgery on speech in the non-cleft population concluded that more evidence is needed as there is no firm conclusion about the effect of orthognathic surgery on speech outcomes.

Studies among the cleft population show inconclusive results concerning the impact of maxillary advancement on VP function. Some studies conclude that maxillary advancement does not lead to negative effects on speech (Nohara et al., 2006; Chua et al., 2010; Pereira et al., 2013; Schultz et al., 2019), while other studies showed worsening of speech condition following the surgery (Haapanen et al., 1997; Trindade et al., 2003; Chanchareonsook et al., 2007; McComb et al., 2011; Impieri et al., 2018; Alaluusua et al., 2019). Variations in results could be attributed to

a difference in study methods such as pre- and post-operative assessment time and assessment methods. Studies had non-homogenous patient groups with varying surgery type, cleft type, pre-operative speech condition, and surgical history. For example, some studies assessed the outcome 3 months after the procedure (Chanchareonsook et al., 2007) while other studies examined the outcome 12-29 months post-operatively (Chua et al., 2010). Select studies failed to report post-operative assessment time (Alaluusua et al., 2019; Schultz et al., 2019). Most studies published utilized perceptual assessment or indirect instrumental assessment of the VP mechanism using the Nasometer (Haapanen et al., 1997; Trindade et al., 2003; Chua et al., 2010; Schultz et al., 2019; Alaluusua et al., 2019) and/or the pressure-flow system (Trindade et al., 2003; Schultz et al., 2019). Direct instrumental assessments include the use of nasopharyngoscopy (Nohara et al., 2006; Chanchareonsook et al., 2007; Chua et al., 2010; McComb et al., 2011), lateral cephalogram (McComb et al., 2011; Impieri et al., 2018), or electromyography (Nohara et al., 2006). Studies thus far have been limited by perceptual, indirect, and superficial methods of assessment without direct visualization of the velopharyngeal musculature before and after maxillary advancement (Sales et al., 2019). Without direct visualization of the musculature, understanding of what factors lead to velopharyngeal insufficiency following maxillary advancement is limited. Visualization of musculature with MRI is needed to examine if changes to the LVP muscle leads to different surgical outcomes.

Orthodontic Treatment and Appliances

As children present with dental anomalies, an evaluation by an orthodontist is necessary. When the child enters mixed dentition, discrepancies in maxillary arch form or transverse width may need to be addressed through maxillary expansion, often using an appliance called quad

helix or Hyrax rapid palatal expander (DiBiase, 2002). Children in mixed and permanent dentition may present with dental crossbites, open bites, rotated teeth, missing teeth, and malocclusions that can be addressed with orthodontic treatment. Orthodontic treatment involves many different parts (see Figure 1.3). Treatment involves the placement of brackets, small metal squares bonded directly to the enamel of the tooth with a special adhesive (Burkey, 2017). Bands, or metal rings, are often used for molar teeth and attached with special dental cement (Burkey, 2017). The arch wire is the wire that connects the brackets and bands together, therefore aligning the teeth. The orthodontist decides how to bend the wire, what size wire to use, and whether additional coil springs are needed on the wire, between certain teeth to achieve appropriate spacing. Once the arch wire is positioned within the bracket, it must be secured in place with elastomeric or stainless-steel ligature. Ligatures can be connected in a row stretched over a group of brackets with a ring going around each bracket, known as a power or energy chain (Sharma, 2017; McDermott, 2022). They can also be individual small rubber rings that hold the arch wire to each bracket, known as "O-rings." Lastly, elastics or rubber bands that stretch from one bracket or band in the upper arch to a bracket or band in the lower arch may be used to provide additional force to move the teeth (Innovative Orthodontic Centers, 2022).

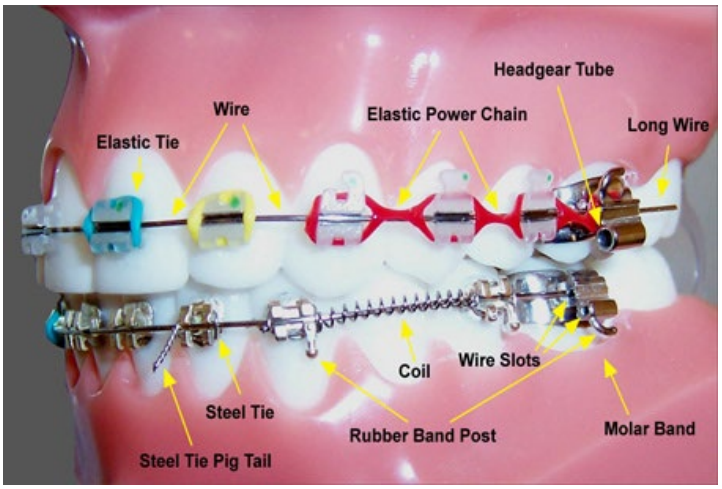

Figure 1.3 Parts of Braces (Yang, 2019)

MRI Considerations in Individuals with Orthodontic Appliances

The largest barrier for the utilization of MRI in imaging for individuals undergoing maxillary advancement is the presence of presurgical orthodontic appliances, often present in cleft patients undergoing this procedure, which could potentially hinder visualization of the velopharyngeal anatomy. MRI involves no radiation exposure as it uses high frequency magnetic field to achieve high contrast between soft tissues. However, the presence of metal objects within the oral cavity can interfere with the image quality and visualization of desired structures. The creation of artifacts due to metals usually lead to areas of signal blackout, due to rims of high signal strength around the object (Gray et al., 2003). Magnetic susceptibility effects could be influenced by MRI parameters such as magnetic field strength, spatial resolution, bandwidth, and TE and echo spacing (Hubalkova et al., 2006). Magnetic susceptibility is the ratio of magnetic response of a material to the applied magnetic field. A greater magnetic field strength creates greater magnetic susceptibility effect, thus causing a more pronounced artifact (Ortiz et al., 1996). The size and shape of the artifact also depends on the magnetic properties of the metal object examined.

Dental and orthodontic appliances are composed of different materials with varying magnetic susceptibility. Previous MRI studies examined the effect of artifacts from orthodontic appliances on visualization of brain structures (Fiala et al., 1994; Shafiei et al., 2003; Hubalkova et al., 2002; Beau, Bossard, & Gebeile-Chauty, 2015). A study using a 1.5 Tesla (1.5T) MR system found that plates made from stainless steel demonstrated the largest artifacts, vitallium plates showed medium artifacts, and titanium plates exhibited the least (Fiala et al., 1994). Another study testing eleven different dental alloys in a 1.5T MRI system using three different sequences demonstrated that commercially pure titanium (Titanium A) and titanium alloys in the

T1 fast-spin echo sequence is least sensitive to metal artifacts (Shafiei et al., 2003). Large artifacts were exhibited in T2 fast-spin echo and gradient echo sequences. In all imaging sequences, alloys composed of palladium and antimony showed no artifact. Hubalkova et al. (2002) reported that dental implants made of pure titanium did not cause visible artifacts, but implants of titanium plus impurities caused medium artifact. Beau et al. (2015) summarized their findings with a chart indicating the recommended procedure for MRI of the oral cavity and other structures in the presence of different orthodontic brackets and retainers (see Figure 1.4). The presence of ceramic brackets, ceramic brackets with cobalt-chromium alloy clip, titanium brackets, and titanium tubes do not interfere with visibility of brain structures in a 1.5T MRI, however, stainless steel brackets and retainers resulted in non-interpretability of the oral cavity (Asano et al., 2016; Beau, Bossard, Gebeile-Chauty, 2015). Further investigation is needed to examine the effect of orthodontic appliances on visualization of velopharyngeal structures using MRI.

Secondly, different metal types may interact with the strong magnetic field resulting in movement to a position pulled by the parallel orientation of magnetic lines of force. Metal constructions used in dentistry contain a wide variety of metals and their alloys. The behavior of the metal object depends on its magnetic properties, such as its magnetic susceptibility. The magnetic susceptibility of a material is dependent on the chemical content of that material and the structure of the elements included (Vikhoff et al., 1995, Beuf et al., 1994; Fache, Price, & Hawbolt, 1987; Shellock & Kanal, 1998). Substances can be diamagnetic, paramagnetic, or ferromagnetic. Diamagnetic substances have the least magnetic susceptibility and are nearly non-magnetic (copper, gold, zinc, lead, carbon, bismuth). Paramagnetic substances cause an increase in effective magnetic field (chromium, manganese, aluminum). Ferromagnetic substances are

strongly attracted by a magnetic field and has the most magnetic susceptibility (iron, cobalt, nickel). Previous studies with brain MRI show that displacement forces induced by magnetic fields on orthodontic appliances are not problematic if the bonding and attachment of the different elements are checked prior to the MRI scan (Kemper et al., 2007; Klocke et al., 2005).

Lastly, the pulsed radiofrequency magnetic field produced by the MR device could result in the heating of metallic objects. Studies of MR procedure-related heating of implants, materials, and devices indicated that minor, negligible temperature changes were observed involving metallic objects (Shellock, 2000; Regier et al., 2009; Kemper et al., 2007; Klocke et al., 2005). In a study with mandibular fixation devices and plates, no detectable temperature change (< 0.1°C) was found in stainless steel, titanium, and vitallium plates (Fiala et al., 1994). Other studies involving metal devices such as implants and aneurysm clips showed that no remarkable temperature rise was found in small metallic implants made of steel or copper clips (Manner et al., 1996). Dempsey and Condon (2001) found normal and extreme temperature changes in medical implants and devices undergoing MRI. Heating effects were greatest in vascular guidewires, with maximal temperature increase up to 72°C. In the reported cases, no patient has been seriously injured because of excessive heat developing in a metallic, implanted device. First-, second-, or third-degree burns associated with devices were reported in monitoring systems due to monitor cables (Shellock, 2000). Additional investigations are warranted to examine the effect of heating for MR systems operating at magnetic field strengths greater than 2.0T (Hubalkova et al., 2006).

It has been reported individuals with cleft anatomy have a higher incidence of dental anomalies compared to the non-cleft population (Jordan et al., 1966; Schroeder & Green, 1975). Dental anomalies are present in approximately 62% of patients with isolated cleft lip and 96.7%

of patients with both cleft lip and palate (Vallino et al., 2008; Akcam et al., 2010). Dental anomalies may include abnormal crown morphology, hypodontia, and supernumerary teeth (Schroeder and Green, 1975; Poyry and Ranta, 1985; Dahllof et al., 1989; Shapira et al., 2000; Dewinter et al., 2003; Ribeiro et al., 2003; Letra et al., 2007; Menezes and Vieira, 2008; Kuchler et al., 2010). It is well documented that the standard orthodontic treatment for the cleft population includes orthodontic treatment during four critical stages: 1) neonatal maxillary orthopedics as an infant with nasoalveolar molding, 2) orthodontic-orthopedic treatment during deciduous dentition, 3) orthodontic treatment during mixed dentition approximately 7-14 years of age, and 4) orthodontic treatment alone or in conjunction with orthognathic surgery of permanent dentition (Machos, 1996). Utilization of a palatal expander is commonly used during stages 2-4 to expand the upper arch that has been collapsed because of scar tissue (Hong & Baek, 2018). During stage 4, orthodontic treatment with the use of brackets, wires, and interarch elastics is often required to achieve decompensation and restore functional occlusion and dentition (Wirthlin & Shetye, 2013). Patients aging 7-18 years undergoing stages 2-4 of orthodontic treatment are also routinely evaluated for velopharyngeal insufficiency (Sie et al., 1998; De Serres et al., 1999; Losken et al., 2003; Inman et al., 2005). Therefore, it is important to know how orthodontic appliances may impact the assessment of the velopharyngeal muscles using MRI.

Figure 1.4 Indications for recommended removal of fixed appliances before MRI scan of head and neck published by Beau, Bossard, & Gebeile-Chauty (2015)

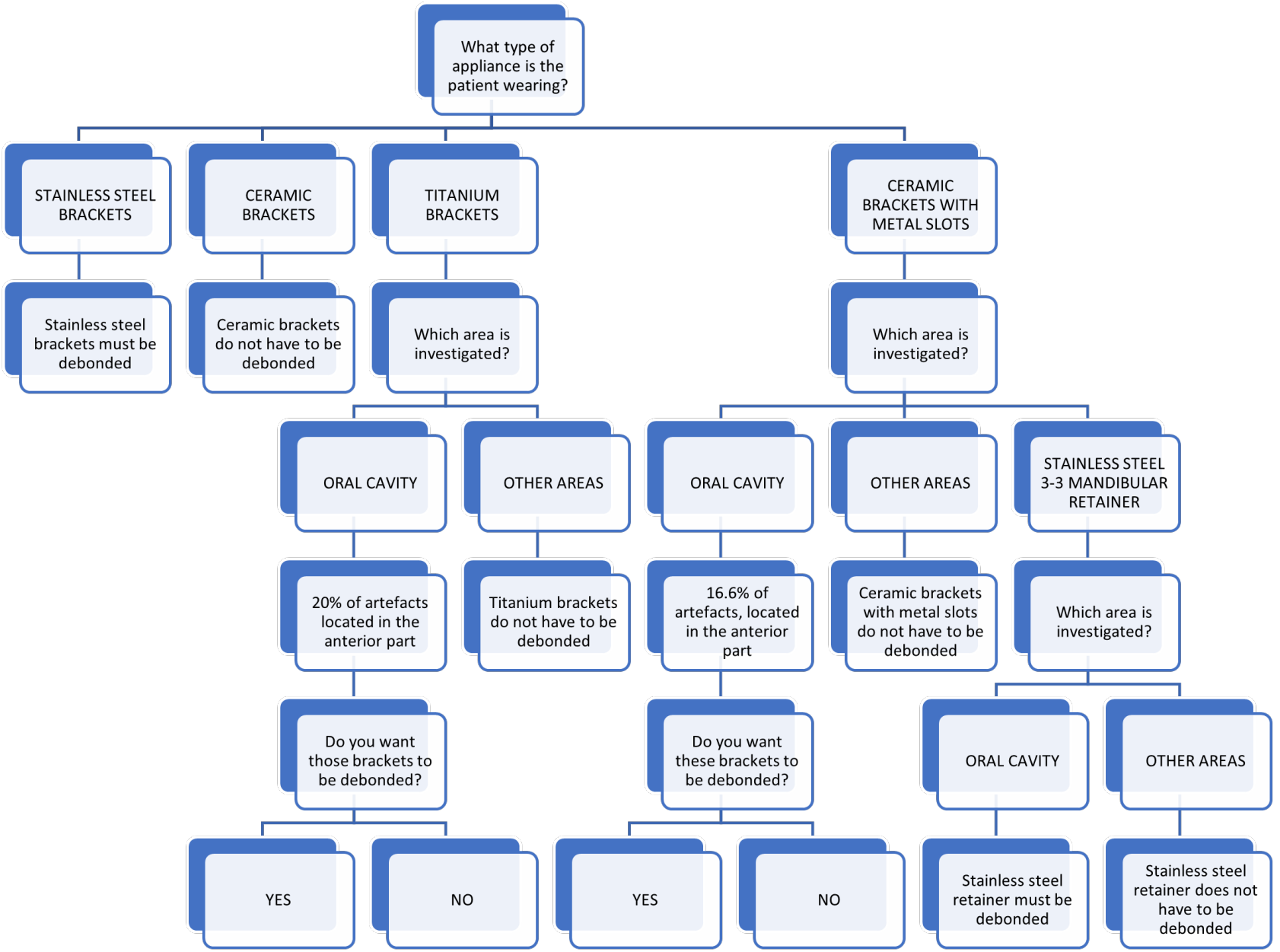

Chapter 2: INTRODUCTION

Magnetic resonance imaging (MRI) is becoming increasingly valuable among cleft palate craniofacial teams in patients with velopharyngeal insufficiency (VPI). It is the only imaging method which allows for direct visualization of the structure and position of the levator veli palatini (LVP) muscle, which is the primary muscle impacted by a cleft palate. A non-sedated, child-friendly imaging protocol has been reported to be successful in 95-100% of children 4 years and older (Kollara & Perry, 2014; Kotlarek et al., 2021). MRI is used in the clinical evaluation process in selected teams throughout the country for patients being considered for surgical management of VPI (Mason & Perry, 2017; Kotlarek et al., 2021). Results of MRI evaluation can be used to guide surgical decisions, such as the insertion site of the sphincter pharyngoplasty surgery (Mason et al., 2021).

Significant findings have been reported in LVP muscle morphology before and after surgery examined using MRI (Perry et al., 2018). Previous studies have utilized MRI to report pre- and post-operative measurements of the LVP features for surgical procedures such as palatoplasty and pharyngoplasty. For example, Kuehn, Ettema, Goldwasser, and Barkmeier (2004) reported findings before and after Furlow double-opposing Z-plasty and V-Y palatoplasty used as primary palatoplasty. Mason (2017) utilized MRI to show changes in tissue following pharyngoplasty. Kotlarek, Perry, and Jaskolka (2022) investigated anatomical changes following the use of pedicled buccal fat pad graft during primary palatoplasty. MRI has also been used to reveal discontinuity of the LVP muscle and absence of a musculus uvulae in children with symptomatic submucous cleft palate (Schenck et al., 2021).

One hindrance to the growing use of MRI among the cleft population is the presence of orthodontic appliances, which could result in image distortions and non-interpretability of MR images. This is particularly a challenge because individuals with cleft anatomy have a higher incidence of dental anomalies compared to the non-cleft population (Jordan et al., 1966; Schroeder & Green, 1975). Dental anomalies are present in approximately 62% of patients with isolated cleft lip and 96.7% of patients with both cleft lip and palate (Vallino et al., 2008; Akcam et al., 2010). Utilization of appliances such as palatal expanders, braces, and wires are needed to address dental anomalies such as abnormal crown morphology, hypodontia, and supernumerary teeth (Schroeder and Green, 1975; Poyry and Ranta, 1985; Dahllof et al., 1989; Shapira et al., 2000; Dewinter et al., 2003; Ribeiro et al., 2003; Letra et al., 2007; Menezes and Vieira, 2008; Kuchler et al., 2010; Hong & Baek, 2018; Wirthlin & Shetye, 2013). Among the cleft population, the most common palatal expanders used are Hyrax or Haas rapid palatal expanders, and quad-Helix (Freitas et al., 2012; Vasant, Menon, & Kannan, 2009; de Almeida et al., 2017; Pugliese et al., 2020). Traditional metal braces composed of stainless-steel brackets and wires are used most frequently for fixed orthodontic treatment (Creekmore & Kunik, 1993; Arici & Regan, 1997; Bazakidou et al., 1997; Maijer & Smith, 1982). Some orthodontists prefer the use of nickel-titanium wires for more favorable biomechanics and elasticity, as well as the use of molar bands and wire spring coils for optimal and effective orthodontic treatment (Kusy & Whitley, 1990; Pandis & Bourauel, 2010; Moresca, Dominguez, & Vigorito, 2011). Patients undergoing orthodontic treatment, often within ages 8-18 years, are also evaluated for VPI and would benefit from an MRI evaluation. However, it is not known how the orthodontic appliances and different dental materials will affect the quality of MR images (Sie et al., 1998; De Serres et al., 1999; Losken et al., 2003; Inman et al., 2005). Because little is known about the impact of orthodontic

devices on VP imaging, MRI is generally assumed to be unavailable as a diagnostic tool while the child is wearing such orthodontic devices. Consequently, the standard approach used at most cleft craniofacial clinics and from the primary mentor's experience as part of a prospective multi-site study (VPI Outcome Predictors Study) at over 14 clinical sites is to disqualify patients with orthodontic appliances from a VP MRI evaluation. However, this limits the use of MRI to evaluate pre- and post-orthognathic surgery outcomes because this is a time period when children with cleft palate will typically be wearing orthodontic devices. To the best of our knowledge, no studies have reported the use of MRI to study the VP muscles using MRI in children with cleft palate before and after orthognathic surgery.

The influence of common orthodontic appliances on the diagnostic quality of MRI of the velopharynx has not been reported. MRI studies of the brain revealed that some appliances and dental materials cause image distortions which result in non-interpretability of MR images, while others do not interfere with visibility of desired structures (Fiala et al., 1994; Shafiei et al., 2003; Hubalkova et al., 2002; Beau, Bossard, & Gebeile-Chauty, 2015). The presence of ceramic brackets, ceramic brackets with cobalt-chromium alloy clip, titanium brackets, and titanium tubes do not interfere with visibility of brain structures in a 1.5T MRI, however, stainless steel brackets and retainers resulted in non-interpretability of the oral cavity (Asano et al., 2016; Beau, Bossard, Gebeile-Chauty, 2015). Titanium, gold, and amalgam was shown to not reduce image quality of MRI sequences used for imaging the oral and maxillofacial region for dental planning (Eggers et al., 2005). Similarly, MRI studies for obstructive sleep apnea report that the extent of artifact and visibility of relevant anatomy varies with different orthodontic appliances (Fleck et al., 2018; Kim, 2018). Donnelly (2005) reported that braces often obscure visualization of the nasopharynx and hypopharynx. Currently, it is not known which orthodontic appliances and

materials hinder visualization of the velopharyngeal structures during an MRI. Therefore, clinicians may be hesitant to refer a child with cleft lip and palate for a VP MRI evaluation. Investigation of the effect of orthodontic appliances on MRI of velopharyngeal structures is necessitated to provide guidance for clinicians referring patients for MRI evaluation. Such insights will provide information about which children with orthodontic devices can be imaged with MRI and allow imaging before and after surgeries (such as orthognathic surgery) that are typically done during ages when children with cleft lip and palate are typically receiving orthodontic care.

This study was designed to evaluate the influence of the most common orthodontic appliances worn by children with cleft lip and palate on VP MRI. We hypothesized that some orthodontic appliances such as Hyrax and quad Helix palatal expanders will not interfere with visibility while others such as stainless-steel brackets and wires will hinder visibility of velopharyngeal muscles. Insights from this study will be useful in determining which patients undergoing orthodontic treatment are candidates for VP MRI.

Chapter 3: METHODS

Participants

In accordance with the East Carolina University institutional review board, 19 participants (7 females, 12 males) aging 11-18 years undergoing stages 2-4 of orthodontic treatment, were recruited at East Carolina University Dental School (Table 3.1). Potential subjects who qualify for participation were provided flyers by the orthodontist at the ECU Dental School. Participants with the following orthodontic appliances were recruited:

I) 1 participant with class II corrector springs,

II) 2 participants with Hyrax palatal expander,

III) 8 participants with stainless steel brackets with Nickel-Titanium wires,

IV) 4 participants with stainless steel brackets with stainless-steel wires, and

V) 4 participants with stainless steel brackets with a combination of Nickel-Titanium and stainless-steel wires.

Subjects with history of claustrophobia, craniofacial anomalies, musculoskeletal disorders, neurological disorders, or anxiety disorder were excluded from this study.

Table 3.1 Participants' demographic information and type of dental appliance.

Subject Code	Appliance Type	Ligature Type	Bands	Upper Archwire	Lower Archwire	Age	Sex	Race	Head Circum. (in.)	Height (in.)	Weight (lbs)
1	A	NA	4	19x25 SS square	19x25 SS square	17	F	Caucasian	22	4'9	104.8
2	B	NA	2	None	None	18	M	African American	22	66.5	183.2
3	B	O-rings	6	018 NiTi Square	17x25 SS Square	15	M	Hispanic	23	68	184.8
4	C	O-rings	1	19x25 NiTi Square	018 NiTi Square	16	M	Arab	22	67	177.2
5	C	O-rings	1	016 NiTi Square	16x22 NiTi Square	15	M	Arab	22.5	69	143
6	C	O-rings	4	19x25 NiTi Square	018 NiTi Square	16	M	Caucasian	22.5	62	101.2
7	C	O-rings	4	17x25 NiTi Square	16x22 NiTi square	11	M	African American	21.75	66	118
8	C	O-rings	0	018 NiTi Square	014 NiTi Square	18	F	Hispanic	21.75	61	151
9	C	O-rings	0	018 NiTi Square	018 NiTi Square	12	F	Caucasian	22	64	200.8
10	C	O-rings	0	018 NiTi Square	16x22 NiTi Square	15	F	Caucasian	21.25	61.5	160.4
11	C	O-rings	0	17x25 NiTi Square	018 NiTi Square	16	F	Caucasian	20.5	64	102.2
12	D	O-rings	4	19x25 SS Square	19x25 SS Square	14	M	African American	22.75	60	98.4
13	D	O-rings	4	19x25 SS Square	19x25 SS Square	14	M	African American	23.75	60	98.6
14	D	O-rings & SS power chain	0	17x25 SS Square	17x25 SS Square	16	M	Caucasian	23.25	69	196.6
15	D	SS power chain	0	17x25 SS Ovoid	17x25 SS Ovoid	15	M	Hispanic	23	66	154.6
16	E	O-rings	2	018 NiTi Square	17x25 SS Square	14	F	Asian	22	61.5	120
17	E	O-rings	4	19x25 NiTi Ovoid	19x25 SS Ovoid	13	M	Mix	22.75	63	153
18	E	O-rings	0	17x25 NiTi Ovoid	17x25 SS Ovoid	15	M	Caucasian	22.75	71	143.6
19	E	O-rings	0	17x25 SS Square with piggy back niti wire of 012	018 NiTi Square	14	F	Hispanic	20	5'2	154.2

*Appliance type: A=class II corrector springs, B=Hyrax palatal expander, C=SS brackets with Ni-Ti wires, D=SS brackets with SS wires, E=SS brackets with combination of Ni-Ti and SS wires; Sex: F=female, M=Male

MRI

All participants were scanned on a 1.5-Tesla Siemens MRI machine with a 12-channel Siemens Trio head coil at the same institution. All participants were scanned in supine position, as differences between upright and supine position has negligible effects on the position and function of the velopharyngeal mechanism (Perry, 2011b; Kollara & Perry, 2014; Broadwell & Perry, 2015; Engwall, 2003). Child-friendly MRI methods previously published was utilized to ensure compliance for the procedure (Kollara et al., 2014; Kollara et al., 2019; Perry et al., 2017; Perry et al., 2018). Two imaging techniques were used:

1) A multi-shot imaging technique using a fast spin-echo (FSE, Table 3.2), also known as rapid acquisition with relaxation enhancement (RARE) or turbo spin echo (TSE). One three-dimensional (3D) scan was obtained at rest, with acquisition time lasting less than 4 minutes (3:59). Then, two-dimensional (2D) scans were taken at rest in the mid-sagittal and oblique coronal plane, each lasting less than 3 minutes. Lastly, two 6-second 2D scans were obtained at the mid-sagittal and oblique coronal plane during sustained phonation of speech sounds /i/ and /s/.
2) A single-shot technique using Half-Fourier Acquisition Single-shot Turbo spin echo (HASTE, Table 3.3) imaging. One three-dimensional (3D) scan was obtained at rest, with acquisition time lasting a little over 5 minutes (5:07). Then, two-dimensional (2D) scans were taken at rest in the mid-sagittal and oblique coronal plane, each lasting 7.9 seconds. Lastly, two 2D scans were obtained at the mid-sagittal and oblique coronal plane during sustained phonation of speech sounds /i/ and /s/, each lasting 7.9 seconds.

Three of the 19 participants were imaged using FSE imaging techniques, and 18 of the 19 participants were imaged using HASTE imaging techniques. MRI data were transferred to Amira 3D v.2021.2 Visualization and Volume modeling software (Thermo Fisher Scientific, Waltham, MA, USA), which includes a native Digital Imaging and Communication in Medicine support (DICOM) program to maintain anatomical geometry when importing images.

Table 3.2 MRI Parameters for the multi-shot imaging technique using a fast spin-echo (FSE)

	3D **FSE**	**Sagittal Rest** **FSE-long**	**Oblique Coronal Rest** **FSE-long**	**Sagittal Rest & Phonation** **FSE**	**Oblique Coronal Rest & phonation** **FSE**
Repetition Time (TR)	2610ms	3000ms	3000ms	987.0ms	987.0ms
Echo Time (TE)	272ms	10ms	10ms	166ms	163ms
Slice thickness	1.00mm	5.0mm	5.0mm	1.5mm	5.0mm
Spacing	0mm	5.0mm	5.0mm	3.5mm	5.0mm
No. of slices	176	23	23	3	3
Length of scan	3:59	2:35	3:11	6.4 sec	6.4 sec
FoV read	192mm	200mm	200mm	160mm	160mm
FoV phase	87.5%	100%	100%	81.3%	81.3%
Voxel Size	1.0x1.0x1.0mm	0.8x0.8x5.0mm	0.8x0.8x5.0mm	1.3x1.3x1.5mm	1.3x1.3x5.0mm

Table 3.3 MRI Parameters for the single-shot technique using Half-Fourier Acquisition Single-shot Turbo spin echo (HASTE)

	T2 SPACE HASTE	**Sag Rest & Phonation**	**OC rest & phonation**
TR	2500ms	1600ms	1600ms
TE	265ms	119ms	119ms
Slice thickness	0.80mm	3.5mm	3.5mm
Spacing	0mm	3.5mm	3.5mm
No. of slices	192	4	4
Length of scan	5:07	7.9 sec	7.9 sec
FoV read	256mm	240mm	240mm
FoV phase	100%	100%	100%
Voxel Size	1.0x1.0x0.8mm	1.3x1.3x3.5mm	1.3x1.3x3.5mm

Assessment of MRI

Images were assessed on a high-resolution monitor independently by one rater with over 4 years of experience in performing MRI evaluations of the velopharynx. The assessment sites were defined at 8 sites that are common landmarks for VP variables and measurements: anterior nasal spine, posterior nasal spine, uvula, posterior pharyngeal wall/adenoid pad, extravelar segment of the LVP, intravelar segment of the LVP, right LVP origin, and left LVP origin. The sites were rated using a score ranging from 1 to 4 for distortion by metal artifacts on MRI with 1 representing "no artifact" and "4" representing "severe distortion" (Asano et al., 2016; Beau, Bossard & Gebeile-Chauty, 2015; Elison et al., 2008; Shalish et al., 2015). Images with scores 1 and 2 are considered "diagnostic" images if the anatomic site can be visualized, even in the presence of distortion. These images can be utilized for diagnostic measurements (Table 3.4). However, images with scores 3 or 4 are considered "moderately diagnostic" or "nondiagnostic" because the level of image distortion is so high that diagnostic measurements cannot be completed for that site. These images are considered non-interpretable by radiologists because at least part of the anatomic site was distorted or subject to a black artifact (Beau, Bossard, & Gebeile-Chauty, 2015). A percentage of images with score 1 or 2 (representing minimal to no artifact) was calculated by type of appliance for each anatomic region.

In addition, images were also assessed based on whether measurements of 8 VP variables could be completed. The VP variables included effective velar length, sagittal angle, hard palate length, velar length, pharyngeal depth, distance of velar knee to posterior pharyngeal wall, LVP muscle length, and LVP muscle origin-to-origin distance (Table 3.5).

Statistical Analysis

Descriptive analysis is reported for the participants' demographic information, ratings at each anatomic site, and VP measurements that were completed. Statistical testing involved the Fisher-Freeman-Halton Exact Test (two-sided) to analyze if differences between orthodontic appliance types, MR imaging techniques, and 3D versus 2D images are statistically significant.

Table 3.4 Distortion Classification

Score	Image Appearance	Diagnostic/nondiagnostic
1	No artifact	Diagnostic
2	Minimal artifact	Diagnostic
3	Moderate artifact	Moderately diagnostic
4	Severe distortion	Nondiagnostic

Images with scores 1 and 2 are considered "diagnostic" images if the anatomic site can be visualized, even in the presence of distortion. Images with scores 3 or 4 reflect images where the level of image distortion is so high that diagnostic measurements cannot be completed for that site. These images are considered non-interpretable by radiologists because at least part of the anatomic site was distorted or subject to a black artifact (Beau, Bossard, & Gebeile-Chauty, 2015).

Table 3.5 Definition of Velopharyngeal Variables of Interest

Variables Measured in the Sagittal Plane	
Hard palate length[1,3,5]	Linear distance between anterior nasal spine and posterior nasal spine
Pharyngeal depth (PNS-PPW) [1,2,3,4,7]	Linear distance (mm) between the posterior nasal spine and posterior pharyngeal wall (PPW) or adenoid at the level of the palatal plane
Velar length[1,2,3,4,7]	Curvilinear distance (mm) from the posterior nasal spine to the uvular tip
Effective velar length[2,3,4,7]	Linear distance (mm) from the posterior nasal spine to the middle of the levator muscle where it inserts into the body of the velum
Sagittal angle [2,7]	Internal angle (degrees) between the plane of the levator muscle and the line coursing through the anterior tubercle of the 3rd and 4th cervical vertebrae
Velar Knee to PPW [7]	Linear distance (mm) from velar knee to the PPW
Variables Measured in the Oblique Coronal Plane	
Levator length[1,2,3,5,6,7,8]	Curvilinear distance (mm) of the levator muscle from the base of the skull (origin) through the midline of the muscle bundle
Origin to origin distance[2,3,5,6,7]	Linear distance (mm) between the two points of origin for the right and left levator muscle bundles

[1] Perry et al., 2014; [2]Kotlarek et al., 2020; [3]Perry, Kotlarek, Sutton, Kuehn, Jaskolka, Fang, Point, Rauccio, 2018; [4]Haenssler, Fang, & Perry, 2020; [5]Perry, Kuehn, Sutton, & Gamage, 2014; [6]Perry, Kuehn, Sutton, 2013; [7]Perry, Kollara, Kuehn, Sutton, & Fang, 2019; [8]Perry, Kuehn, Sutton, & Fang, 2017

CHAPTER 4: RESULTS

Results of MRI Assessment by Appliance Type (Figure 4.1)

In imaging with Class II Corrector springs (type A), all 8 of the anatomic regions were affected by metal resulting in a distortion score of 3 or 4 (Table 4.3). Consequently, none of the VP variables was able to be measured since the landmarks were moderately or severely distorted (Table 4.4). MR imaging in the VP region would be infeasible for this appliance.

In imaging with Hyrax palatal expander (type B), only one anatomic region, the posterior nasal spine, consistently resulted in a distortion score of 3 or 4 (Table 4.3). Another anatomic region, the anterior nasal spine, had minimal artifact for Participant 2 but severe distortion for Participant 3. This is likely attributed to the difference between distortion caused by Hyrax palatal expander alone (Participant 2) versus distortion caused by Hyrax palatal expander with braces (Participant 3). All other 6 anatomic regions displayed minimal to no artifact by metal. Only three of the eight VP variables (distance between velar knee to posterior pharyngeal wall, LVP muscle length, distance between LVP origins) were able to be measured since landmarks for other variables were moderately or severely distorted (Table 4.4).

In imaging with stainless-steel brackets and Nickel-Titanium wires (type C), two of the anatomic regions, the anterior nasal spine and posterior nasal spine, resulted in a distortion score of 3 or 4 for majority of participants in the group. Four anatomic regions (uvula, posterior pharyngeal wall, right LVP origin, and left LVP origin) displayed minimal to no artifact by metal. The intravelar and extravelar segments of the LVP displayed minimal to no artifact for 87.5% of the participants with type C appliance. Only three of the eight VP variables (distance between velar knee to posterior pharyngeal wall, LVP muscle length, distance between LVP

origins) were able to be measured for all participants (Table 4.4). For one participant (Participant 6), the sagittal angle was able to be measured.

In imaging with stainless-steel brackets and stainless-steel wires (type D), two of the anatomic regions, the anterior nasal spine and posterior nasal spine, resulted in a distortion score of 3 or 4 for all participants in the group. The other six anatomic regions were unaffected by the appliance. Only three of the eight VP variables (distance between velar knee to posterior pharyngeal wall, LVP muscle length, distance between LVP origins) were able to be measured for all participants (Table 4.4). For one participant (Participant 13), the sagittal angle was able to be measured.

The last group consisted of participants with stainless-steel brackets and a combination of Nickel-Titanium and stainless-steel wires (type E). Two of the anatomic regions, the anterior nasal spine and posterior nasal spine, resulted in a distortion score of 3 or 4 for all participants in the group. The intravelar segment of the LVP displayed minimal to no artifact for 66.7% of the participants with type E appliance. The other five anatomic regions were unaffected by the appliance. Only three of the eight VP variables (distance between velar knee to posterior pharyngeal wall, LVP muscle length, distance between LVP origins) were able to be measured for all participants (Table 4.4). For one participant (Participant 17), the sagittal angle was able to be measured.

Results of the Fisher-Freeman-Halton Exact Test (two-sided) showed no statistically significant difference ($p > 0.05$) between the five appliance groups for artifact by anatomic region (Table 4.3) and measurability of velopharyngeal variables (Table 4.4).

Table 4.1 Results of Velopharyngeal Variables of Interest by Appliance Type and MRI Sequence

Subject No.	Appliance Type	MRI Sequence	Effective velar length (PNS-LVP)	Sagittal Angle	Hard palate length	Velar Length	Pharyngeal depth (PNS-PPW)	Velar knee to PPW	LVP muscle length	LVP muscle O-to-O_rest
1	A	HASTE	No	No	No	No	No	No	No	No
2	B	HASTE	No	No	No	No	No	Yes	Yes	Yes
3	B	HASTE	No	No	No	No	No	Yes	Yes	Yes
4	C	FSE	No	No	No	No	No	No	No	No
4	C	HASTE	No	No	No	No	No	Yes	Yes	Yes
4	C	FSE-long	---	---	No	No	No	Yes	No	Yes
5	C	HASTE	No	No	No	No	No	Yes	Yes	Yes
6	C	HASTE	No	Yes	No	No	No	Yes	Yes	Yes
7	C	FSE	No	No	No	No	No	Yes	No	No
7	C	HASTE	No	No	No	No	No	Yes	Yes	Yes
8	C	HASTE	No	No	No	No	No	Yes	Yes	Yes
9	C	HASTE	No	No	No	No	No	Yes	Yes	Yes
10	C	HASTE	No	No	No	No	No	Yes	Yes	Yes
11	C	HASTE	No	No	No	No	No	Yes	Yes	Yes
12	D	HASTE	No	No	No	No	No	Yes	Yes	Yes
13	D	HASTE	No	Yes	No	No	No	Yes	Yes	Yes
14	D	HASTE	No	No	No	No	No	Yes	Yes	Yes
15	D	HASTE	No	No	No	No	No	Yes	Yes	Yes
16	E	HASTE	No	No	No	No	No	Yes	Yes	Yes
17	E	HASTE	No	Yes	No	No	No	Yes	Yes	Yes
18	E	HASTE	No	No	No	No	No	Yes	Yes	Yes
19	E	FSE	No	No	No	No	No	No	No	No
19	E	FSE-long	---	---	No	No	No	Yes	No	Yes

*Appliance type: A=class II corrector springs, B=Hyrax palatal expander, C=SS brackets with Ni-Ti wires, D=SS brackets with SS wires, E=SS brackets with combination of Ni-Ti and SS wires

*Yes=Able to measure successfully, No=Unable to measure successfully

Table 4.2 Results of the Anatomic Regions of Interest by Appliance Type and MRI Sequence

Subject No.	Appliance Type	MRI Sequence	ANS	PNS	Uvula	PPW or adenoid	Extravelar segment of LVP	Intravelar segment of LVP	Right LVP origin	Left LVP origin
1	A	HASTE	4	4	4	3	3	4	3	4
2	B	HASTE	2	4	1	1	1	1	1	1
3	B	HASTE	4	3	1	1	2	2	1	1
4	C	FSE	4	4	2	2	4	4	4	4
4	C	HASTE	4	3	1	1	1	1	1	1
4	C	FSE-long	4	4	2	2	2	3	1	1
5	C	HASTE	4	4	2	1	1	2	1	1
6	C	HASTE	4	2	1	1	1	2	1	1
7	C	FSE	4	3	1	1	4	4	3	3
7	C	HASTE	4	3	1	1	1	1	1	1
8	C	HASTE	4	3	1	1	1	1	1	1
9	C	HASTE	4	4	1	1	1	1	1	1
10	C	HASTE	4	3	1	1	2	2	1	2
11	C	HASTE	4	4	2	1	3	3	2	1
12	D	HASTE	4	3	1	1	2	2	2	1
13	D	HASTE	4	4	1	1	1	1	2	1
14	D	HASTE	4	3	1	1	2	1	1	2
15	D	HASTE	4	3	1	1	1	1	1	1
16	E	HASTE	4	3	1	1	1	2	1	1
17	E	HASTE	4	3	1	1	1	2	1	1
18	E	HASTE	4	3	2	1	1	3	1	1
19	E	FSE	4	4	3	3	4	4	4	4
19	E	FSE-long	4	4	2	1	1	2	1	1

*Appliance type: A=class II corrector springs, B=Hyrax palatal expander, C=SS brackets with Ni-Ti wires, D=SS brackets with SS wires, E=SS brackets with combination of Ni-Ti and SS wires

*1=no artifact, 2=minimal artifact, 3=moderate artifact, 4=severe distortion

Table 4.3 Percentage of score 1 or 2 images with metal artifacts by type of appliance for each anatomic region using HASTE MRI sequence.

	Class II corrector springs		Hyrax palatal expander		SS brackets with Ni-Ti wires		SS brackets with SS wires		SS brackets with combination of Ni-Ti & SS wires		Fisher-Freeman-Halton Exact Test
	Group A		Group B		Group C		Group D		Group E		2-sided (p-value)
Anatomic region	n=1		n=2		n=8		n=4		n=3		
Anterior nasal spine	0	0%	1	50%	0	0%	0	0%	0	0%	0.167
Posterior nasal spine	0	0%	0	0%	1	12.50%	0	0%	0	0%	0.451
Uvula	0	0%	2	100%	8	100%	4	100%	3	100%	0.056
Posterior pharyngeal wall	0	0%	2	100%	8	100%	4	100%	3	100%	0.056
Extravelar segment of LVP	0	0%	2	100%	7	87.50%	4	100%	3	100%	0.268
Intravelar segment of LVP	0	0%	2	100%	7	87.50%	4	100%	2	66.70%	0.235
Right LVP origin	0	0%	2	100%	8	100%	4	100%	3	100%	0.056
Left LVP origin	0	0%	2	100%	8	100%	4	100%	3	100%	0.056

Table 4.4 Results of Velopharyngeal Variables of Interest by Appliance Type

Type of Appliance	Effective velar length (PNS-LVP)	Sagittal Angle	Hard palate length (ANS-PNS)	Velar Length (PNS-Uvula)	Pharyngeal depth (PNS-PPW)	Velar knee to PPW	LVP muscle length	LVP muscle O-to-O
Class II corrector springs								
Hyrax palatal expander						✓	✓	✓
SS brackets with Ni-Ti wires		✓ [12.5%]				✓	✓	✓
SS brackets with SS wires		✓ [25%]				✓	✓	✓
SS brackets with combination of Ni-Ti & SS wires		✓ [33%]				✓	✓	✓
Fisher-Freeman-Halton Exact test (two-sided p-value)	NA	0.863	NA	NA	NA	0.056	0.056	0.056

*Check mark indicates variables that can be measured. Percentage below the check mark indicates the percentage of participants with MR images that could be measured for that variable. No check mark indicates the variable could not be measured. NA indicates statistical analysis was completed because the outcome variable was a constant between groups.

Figure 4.1 Example of MR images by MRI scan and appliance type

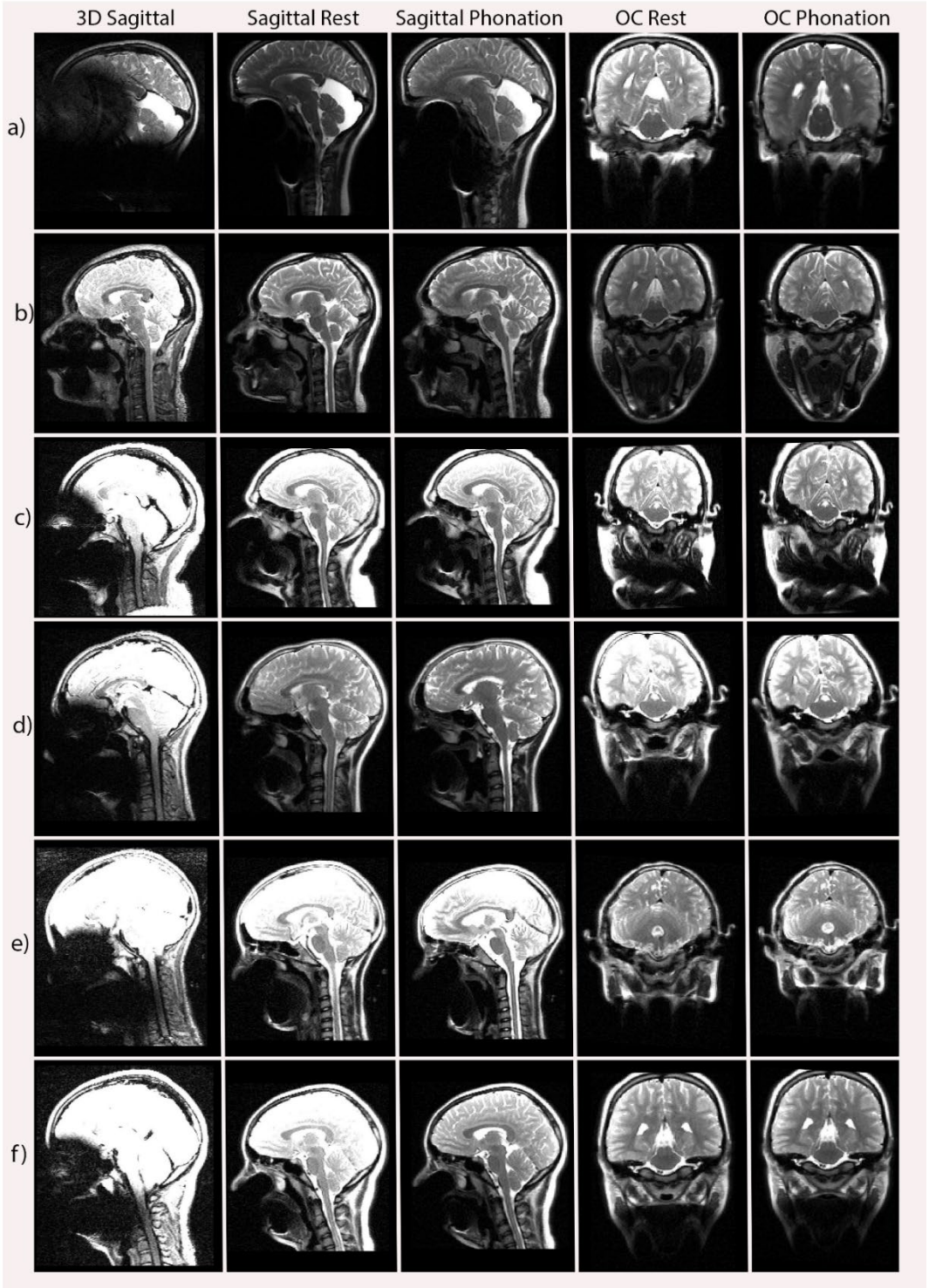

*Appliance type by rows: a) class II corrector springs, b) hyrax palatal expander, c) hyrax palatal expander with braces, d) stainless steel (SS) brackets with SS wires, e) SS brackets with nickel-titanium (Ni-Ti) wires, f) SS brackets with combination of SS and Ni-Ti- wires

MRI Sequence Type

In imaging using the HASTE MR imaging technique, six of the eight anatomic regions resulted in minimal to no artifact by metal (Table 4.5). In imaging using the FSE MR imaging technique, only two of the eight anatomic regions resulted in minimal to no artifact by metal. It was also noted that MR sequences with longer acquisition times (2-3 minutes) for the FSE MR imaging technique resulted in decreased metal artifact and image distortion (Figure 4.2). However, MRI scans during sustained phonation were not able to be acquired with the longer acquisition times using FSE, as the participant is not able to produce a sustained speech sound for 2-3 minutes. Consequently, only one VP variable was successfully measured using the FSE MR imaging technique compared with the four VP variables that was successfully measured for the HASTE MR imaging technique (Table 4.6). It is recommended that MR imaging in the VP region should utilize the HASTE MR imaging technique.

Results of the Fisher-Freeman-Halton Exact Test (two-sided) showed a statistically significant difference ($p < 0.05$) between the three MRI sequence groups for six of eight anatomic regions (Table 4.5) and three of eight velopharyngeal variables (Table 4.6).

Table 4.5 Percentage of score 1 or 2 images with metal artifacts by MRI sequence type for each anatomic region.

Anatomic region	FSE		FSE-long		HASTE Group C & E		Fisher-Freeman-Halton Exact Test
	n=3		n=2		n=11		2-sided (p-value)
Anterior nasal spine	0	0%	0	0%	0	0%	NA
Posterior nasal spine	0	0%	0	0%	1	9.1%	1.000
Uvula	2	66.7%	2	100%	11	100%	0.002*
Posterior pharyngeal wall	2	66.7%	2	100%	11	100%	0.033*
Extravelar segment of LVP	0	0%	2	100%	10	90.9%	0.009*
Intravelar segment of LVP	0	0%	1	50%	9	81.8%	0.005*
Right LVP origin	0	0%	2	100%	11	100%	0.002*
Left LVP origin	0	0%	2	100%	11	100%	0.002*

*notates statistically significant difference ($p<0.05$)

Table 4.6 Results of Velopharyngeal Variables of Interest by MRI sequence

MRI Protocol	Effective velar length (PNS-LVP)	Sagittal Angle	Hard palate length (ANS-PNS)	Velar Length (PNS-Uvula)	Pharyngeal depth (PNS-PPW)	Velar knee to PPW	LVP muscle length	LVP muscle O-to-O
FSE						✓ [33%]		
FSE-long	NA	NA				✓		✓
HASTE		✓ [18%]				✓	✓	✓
Fisher-Freeman-Halton Exact test (two-sided p-value)	NA	1.000	NA	NA	NA	0.033*	<0.001*	0.002*

*notates statistically significant difference ($p<0.05$)

Figure 4.2 Example of MR images comparing three different MR imaging sequences for Participant 4.

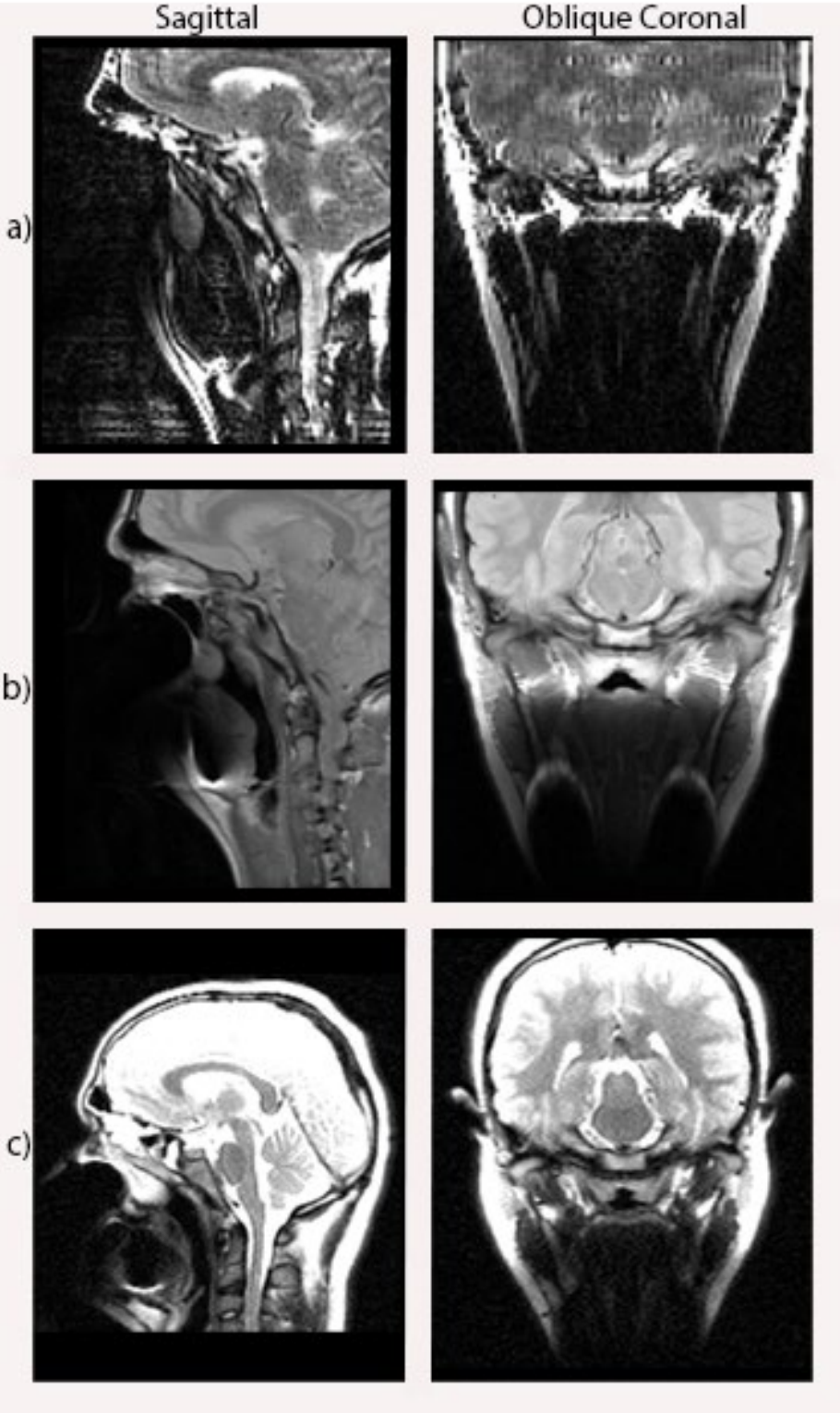

*MR imaging sequence type by rows: a) FSE, b) FSE long, c) HASTE

MRI Scan Type (Figure 4.3)

In imaging where a three-dimensional (3D) image is acquired, all of the anatomic regions of interest resulted in moderate to severe distortion for at least 50% of participants due to the metal artifact (Table 4.7). In imaging where a two-dimensional (2D) image is acquired, only two of the eight anatomic regions resulted in moderate to severe distortion from metal artifact. Three VP variables were successfully measured for 94% of participants using the 2D images compared with only 11-17% of participants using the 3D images acquired (Table 4.8). It is recommended that MR imaging in the VP region should utilize 2D image acquisition protocols.

Results of the Fisher-Freeman-Halton Exact Test (two-sided) showed a statistically significant difference ($p < 0.05$) between 3D and 2D MR images for six of eight anatomic regions (Table 4.7) and three of eight velopharyngeal variables (Table 4.8).

Table 4.7 Percentage of score 1 or 2 images with metal artifacts for 3D versus 2D MR images for each anatomic region.

Anatomic region	3D		2D		Fisher-Freeman-Halton Exact Test 2-sided (p-value)
	n=18		n=18		
Anterior nasal spine	0	0%	0	0%	1.00
Posterior nasal spine	0	0%	0	0%	1.00
Uvula	1	5.6%	17	94.4%	<0.001*
Posterior pharyngeal wall	2	11.1%	17	94.4%	<0.001*
Extravelar segment of LVP	6	33.3%	16	88.9%	0.002*
Intravelar segment of LVP	3	16.7%	16	88.9%	<0.001*
Right LVP origin	8	44.4%	17	94.4%	0.003*
Left LVP origin	9	50%	17	94.4%	0.007*

*notates statistically significant difference (p<0.05)

Table 4.8 Results of Velopharyngeal Variables of Interest for 3D versus 2D MR images

MRI Protocol	Effective velar length (PNS-LVP)	Sagittal Angle	Hard palate length (ANS-PNS)	Velar Length (PNS-Uvula)	Pharyngeal depth (PNS-PPW)	Velar knee to PPW	LVP muscle length	LVP muscle O-to-O
3D		✓ [17%]				✓ [11%]	✓ [17%]	✓ [17%]
2D		NA				✓ [94%]	✓ [94%]	✓ [94%]
Fisher-Freeman-Halton Exact test (two-sided p-value)	NA	NA	NA	NA	NA	<0.001*	<0.001*	<0.001*

*notates statistically significant difference ($p<0.05$)

NA = could not be calculated

Figure 4.3 Example of 3D and 2D MR images for participant 16.

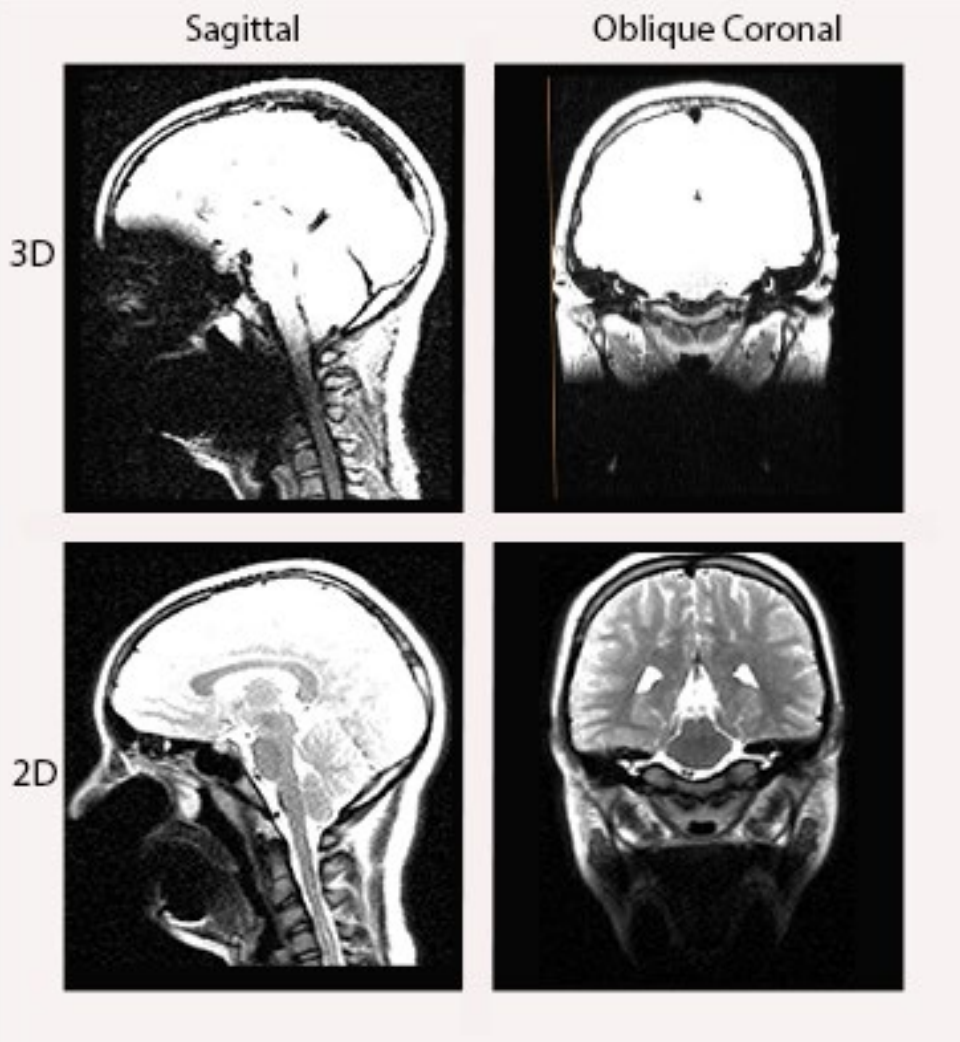

Molar Bands

Of the 15 participants with braces (Type C, D, & E), 7 participants had no molar bands, two participants had one molar band, one participant had two molar bands, and five participants had four molar bands. Six of the eight anatomic regions resulted in minimal to no artifact by metal for majority of participants in all groups (Table 4.9). For all groups, three VP variables was successfully measured for all participants (Table 4.10). Of the five participants with four molar bands, three participants had images that resulted in successful measurement of the sagittal angle variable. Based on the results, it is likely that the number of molar bands do not contribute to distortion and artifact in MR imaging in the VP region.

Results of the Fisher-Freeman-Halton Exact Test (two-sided) showed no statistically significant difference ($p > 0.05$) between the number of molar bands for artifact by anatomic region (Table 4.9) and measurability of velopharyngeal variables (Table 4.10).

Table 4.9 Percentage of score 1 or 2 images with metal artifacts by number of molar bands for each anatomic region.

Anatomic region	No Molar Bands n=7		1 Molar Band n=2		2 Molar Bands n=1		4 Molar bands n=5		Fisher-Freeman-Halton Exact Test 2-sided (p-value)
Anterior nasal spine	0	0%	0	0%	0	0%	0	0%	NA
Posterior nasal spine	0	0%	0	0%	0	0%	1	20%	0.533
Uvula	7	100%	2	100%	1	100%	5	100%	NA
Posterior pharyngeal wall	7	100%	2	100%	1	100%	5	100%	NA
Extravelar segment of LVP	6	85.6%	2	100%	1	100%	5	100%	1.000
Intravelar segment of LVP	5	71.4%	2	100%	1	100%	5	100%	0.667
Right LVP origin	7	100%	2	100%	1	100%	5	100%	NA
Left LVP origin	7	100%	2	100%	1	100%	5	100%	NA

Table 4.10 Results of Velopharyngeal Variables of Interest by number of molar bands

Other Appliances	Effective velar length (PNS-LVP)	Sagittal Angle	Hard palate length (ANS-PNS)	Velar Length (PNS-Uvula)	Pharyngeal depth (PNS-PPW)	Velar knee to PPW	LVP muscle length	LVP muscle O-to-O
No molar bands (n = 7)						✓	✓	✓
1 molar band (n = 2)						✓	✓	✓
2 molar bands (n = 1)						✓	✓	✓
4 molar bands (n = 5)		✓ [60%]				✓	✓	✓
Fisher-Freeman-Halton Exact test (two-sided p-value)	NA	0.095	NA	NA	NA	NA	NA	NA

Wire Spring Coil

Three participants had a spring coil on the wire (Participants 9, 11, 18). Two of the participants had a spring coil on type C appliance and one of the participants had a spring coil on type E appliance. Participants with type C and type E appliance were organized into four groups for comparison. Six of the eight anatomic regions resulted in minimal to no artifact by metal for majority of participants in all groups (Table 4.11). For all groups, three VP variables was successfully measured for all participants (Table 4.12). Two participants without spring coils had images that resulted in successful measurement of the sagittal angle variable. Based on the results, it is likely that the presence of spring coils does not contribute to distortion and artifact in MR imaging in the VP region.

Results of the Fisher-Freeman-Halton Exact Test (two-sided) showed no statistically significant difference ($p > 0.05$) between the presence and absence of a wire spring coil for artifact by anatomic region (Table 4.11) and measurability of velopharyngeal variables (Table 4.12).

Table 4.11 Percentage of score 1 or 2 images with metal artifacts by presence/absence of a wire spring coil for each anatomic region.

Anatomic region	With Spring Coil Type C & E		Without Spring Coil Type C & E		Fisher-Freeman-Halton Exact Test
	n=3		n=8		2-sided (p-value)
Anterior nasal spine	0	0%	0	0%	NA
Posterior nasal spine	0	0%	1	12.5%	1.000
Uvula	3	100%	8	100%	NA
Posterior pharyngeal wall	3	100%	8	100%	NA
Extravelar segment of LVP	2	66.7%	8	100%	0.455
Intravelar segment of LVP	2	66.7%	7	87.5%	0.182
Right LVP origin	3	100%	8	100%	NA
Left LVP origin	3	100%	8	100%	NA

Table 4.12 Results of Velopharyngeal Variables of Interest for participants with and without a wire spring coil

Other Appliances	Effective velar length (PNS-LVP)	Sagittal Angle	Hard palate length (ANS-PNS)	Velar Length (PNS-Uvula)	Pharyngeal depth (PNS-PPW)	Velar knee to PPW	LVP muscle length	LVP muscle O-to-O
Type C with spring coil (n = 2)						✓	✓	✓
Type C without spring coil (n = 6)		✓ [18%]				✓	✓	✓
Type E with spring coil (n = 1)						✓	✓	✓
Type E without spring coil (n = 2)		✓ [50%]				✓	✓	✓
Fisher-Freeman-Halton Exact test (two-sided p-value)	NA	0.727	NA	NA	NA	NA	NA	NA

Chapter 5: DISCUSSION

Velopharyngeal Variables and Anatomic Sites

For all appliance types, the two anatomic sites that resulted in most severe distortion from artifact by metal was the anterior nasal spine and the posterior nasal spine (PNS). The distortion of the PNS is notable because this site is the landmark for four of the eight key VP variables used in evaluation of VP using MRI. The range distance of distortion for 2D MRI scans in the present study extended posteriorly 53-69mm from the pronasale (PRN), most anterior point of the nose. The inability to visualize the PNS hinders analysis of several VP variables commonly measured and used in VP MRI studies, including the hard palate length, velar length, effective velar length, and pharyngeal depth (Figure 5.1). There are two possible solutions to this problem: 1) utilize an alternative imaging method in addition to MRI to obtain these measures distorted by metal in an MRI evaluation, 2) utilize another anatomic site to estimate the location of the PNS to measure the needed VP variables. The first solution may be more feasible and most reliable; however, this will require collaboration with the orthodontic or dental team, as routine lateral cephalograms are often performed as a part of dental protocol. Numerous studies have demonstrated successful measurement of hard palate length, velar length, and pharyngeal depth using lateral cephalograms (Subtelny, 1957; Wu et al., 1996; Satoh et al., 2004; Satoh et al., 2005; You et al., 2008; Gohilot et al., 2014). However, while some studies have attempted to describe effective velar length using cephalograms (Calnan, 1961; Mason, 1969), others argue that effective velar length is most accurately measured using MRI because it allows for precise in-plane measure of the center of the LVP muscle (Tian & Redett, 2009; Haenssler, Fang, & Perry, 2020). Therefore, a combination of both imaging methods may be required. Critical landmarks, such as the anterior nasal spine, posterior nasal spine, sella turcica, and nasion, can be traced in the lateral

cephalogram then superimposed on the sagittal MR image (Figure 5.2). The second solution has been explored by a handful of studies but has yet to show high reliability ratings. For individuals with repaired cleft of the hard palate, the PNS is non-existent. Therefore, the posterior nasal spine landmark can be determined by the bony terminal end of the hard palate intersected by the midsagittal line identified by observing axial MRI scans of the palate (Tian et al., 2010; Perry et al., 2018). Other studies suggest that other landmarks, such as the pterygomaxillary fissure, could be utilized to trace the point of the PNS (Krogman et al., 1975; Hotz & Gnoinski, 1976; Rygh & Sirinavin, 1982; Tindlund et al., 1993; Bongaarts et al., 2008). The PNS can be approximated by extending the lowest point on the pterygomaxillary fissure, between the anterior margin of the pterygoid process and the posterior margin of the maxillary tuberosity, until it intersects the palatal plane (Krogman et al., 1975; Lu et al., 2006). More normative data is needed to utilize the posterior hard palate as an anatomic landmark in the non-cleft population for clinical comparisons to be readily available.

For all participants with appliance types B-E, three VP variables were able to be successfully measured (distance from velar knee to PPW, LVP length, and LVP origin distance). This is a valuable finding because these VP variables alone could provide critical clinical information to guide surgical intervention. Recent findings in MRI evaluation report significant differences in LVP length and LVP origin distance between individuals with normal anatomy and individuals with velopharyngeal dysfunction (VPD). Individuals with cleft anatomy present with a larger pharyngeal depth, shorter LVP length, narrower LVP origin distance (Kollara et al., 2017; Filip et al., 2018; Kollara et al., 2019; Haenssler et al., 2020). Similarly, individuals with 22q11.2 deletion syndrome, who present with a 74-97% incidence rate of VPI, also present with shorter LVP length and narrower LVP origin distance compared to individuals with

velopharyngeal competence and normal anatomy (Lipson et al., 1991; Rommel et al., 1999; Solot et al., 2001; Shprintzen, 2008). While other VP variables may be distorted by metal of orthodontic appliances, visibility of these three VP variables warrant an MRI evaluation for individuals presenting with VPD.

It is important to consider why some anatomic sites are negatively impacted and why some are not. Given the placement of the orthodontic appliances, structures of the hard palate and anterior soft palate are in closer proximity to the metal, therefore causing more severe distortion. Structures such as the uvula and posterior pharyngeal wall are in farther proximity of the dental appliances, resulting in higher visibility. Similarly, the structures of the LVP muscle are posterior and superior to the metal appliance, therefore have the greatest visibility. However, it is notable that the intravelar segment of the LVP is more likely to be distorted than the extravelar segment, likely because it is located more inferiorly and in closer proximity to the metal appliance. Past MRI studies suggest that dental appliances may cause less than 30 mm^2 radius of distortion, which is similar to what was observed in the present study (Klinke et al., 2012).

Figure 5.1

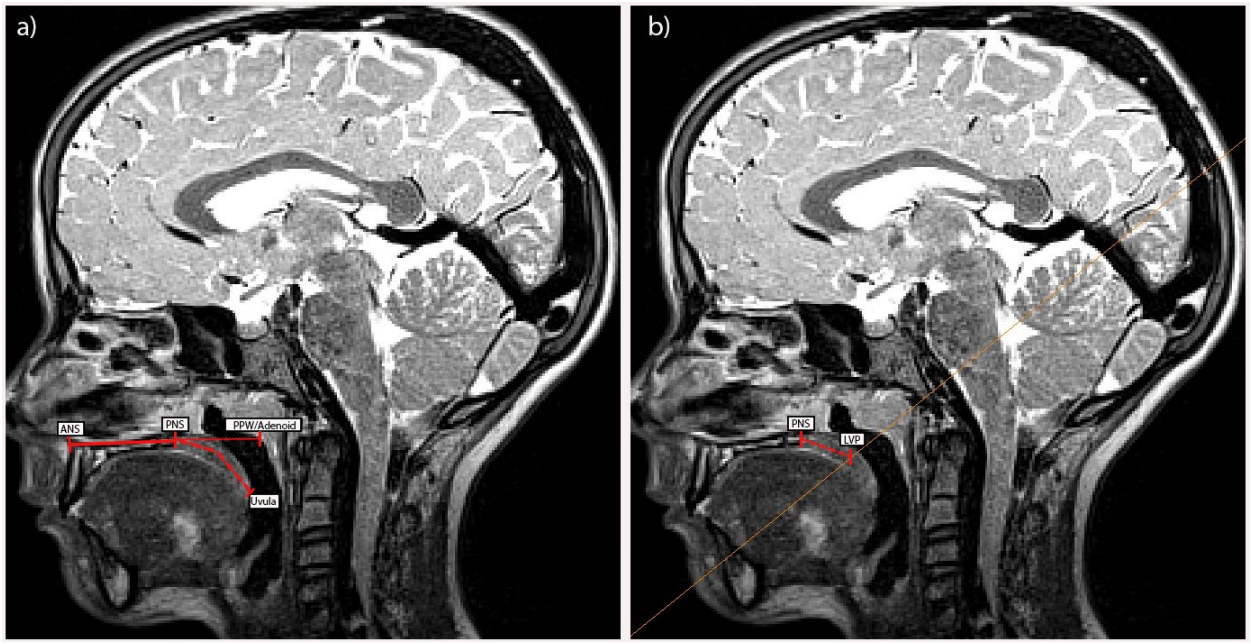

Velopharyngeal variables involving PNS (a) ANS to PNS: hard palate length, PNS to PPW/adenoid: pharyngeal depth, PNS to Uvula: velar length (b) PNS to LVP (intersected by oblique coronal plane): effective velar length

Figure 5.2

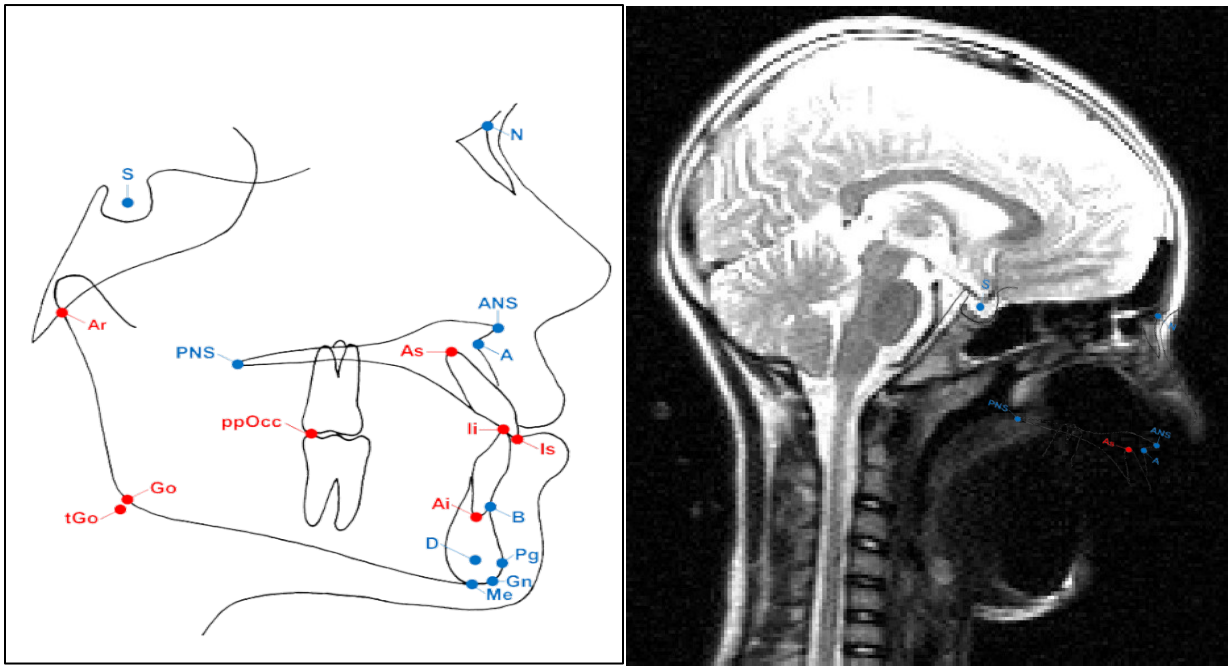

Example of how landmarks can be traced on a lateral cephalogram (left) then superimposed on an MR image to provide information needed to complete VP variable measurements of interest.

Dental Materials

The present study separated individuals with three different wire types – nickel-titanium, stainless steel, and combination of both materials. However, no statistically significant difference was found between the three groups. This is a novel finding because previous literature suggested removal of appliances that contained stainless steel brackets and wires (Asano et al., 2016; Beau, Bossard, Gebeile-Chauty, 2015). However, previous studies did not examine the same anatomic sites and VP variables as in the present study. In addition, additional metal parts such as molar bands and wire spring coils did not contribute to increased distortion.

Class II corrector spring was the outlier. No statistical significance was found between the appliance groups, which could be attributed to the low power of the group with class II corrector springs due to the small sample size (n = 1). Findings from MRI scans were clinically significant because all anatomic sites were severely distorted and VP variables could not be measured (Figure 4.1 and Table 4.3, 4.4). The composition of the correct springs was stainless steel inner shaft/push rod, middle and outer tubing, with a nickel-titanium spring (American Orthodontics, 2021). This is important because other appliances not included in this study, such as plates and screws could result in the severe distortion and would not validate an MRI evaluation of the VP mechanism. However, only one participant with this appliance was recruited and could be an outlier. Further exploration is needed to confirm the findings of this study with this appliance type.

One participant among the type C appliance group (Participant 8) had an amalgam filling on the maxillary right second molar (tooth #31). This did not result in any increased distortion of the LVP intravelar segment compared with other participants. Amalgam is a material composed of a mixture of metals, including liquid mercury and a powdered alloy composed of silver, tin,

and copper (United States Federal Food & Drug Administration, 2021). Previous studies reported that amalgam fillings resulted in no imaging artifacts for MRI of head and neck (Hinshaw et al., 1988; Abbaszadeh, Heffez, & Mafee, 2000; Gray, Redpath, & Smith, 1996; Starčuková et al., 2008). Similarly, the findings of this study suggest that amalgam fillings do not interfere with visualization of the LVP, however further examination is needed with different size, location, and number of amalgam fillings.

Another appliance part worth addressing is orthodontic ligatures, which function to tie the brackets and wires together. Ligatures can be made up of rubber or stainless steel and can tie each bracket individually known as "O-ties" or "O-rings" or can tie a row of brackets together known as "power chain" or "energy chain." Some ligatures made up of rubber may be metallic in color while others are made up of stainless steel. The present study included only participants with ligatures made up of rubber. Further examination is needed to determine if the presence of stainless-steel power chain ligatures interfere with MRI evaluation of the VP mechanism.

MRI Sequence Type

The main difference between the FSE and the HASTE imaging techniques is that FSE is a multi-shot technique and HASTE is a single-shot technique. Multi-shot techniques are more common for most clinical applications, especially for T2-weighted images, because it acquires multiple spin echoes per excitation pulse and thus reduces the duration of each shot (Cohen & Mitchell, 2004). However, multi-shot image is more sensitive to motion (Cohen & Mitchell, 2004). Single shot techniques obtain one spin echo or signal per excitation pulse. Improved implementation of the single shot techniques, such as the HASTE, use high-speech imaging gradients and partial-Fourier techniques to refocus after every echo, resulting in relative

insensitivity and susceptibility to artifacts (Patel et al., 1997). However, the refocusing results in increased time per shot.

The majority of recently published MRI studies of individuals without dental and orthodontic appliances has been successful with a turbo-spin-echo (TSE) sequence, another term for FSE (Beer et al., 2004; Tian et al., 2010; Perry, Kuehn, & Sutton, 2016; Perry et al., 2017; Mason, Pua, & Perry, 2018; Kollara et al., 2019; Kotlarek, Haenssler, Hildebrand, Perry, 2019; Kotlarek et al., 2022; Haenssler, Perry, Mann & Mann, 2021). The same FSE sequence used in this study has been successfully reported during sustained phonation in individuals without dental and orthodontic appliances (Kollara, Perry, & Hudson, 2016; Mason, Pua, & Perry et al., 2018; Kollara et al., 2022). A handful of studies two decades ago report the use of a fast gradient-echo sequence with echo-planar imaging (Wein et al., 1991; Suto et al., 1993; Gilbert et al., 1998; Anagnostara et al., 2001). To our knowledge, no previous studies have reported the use of HASTE sequence for individuals underdoing VP MRI.

These two MR imaging techniques were used in the present study because the FSE technique is most reported in recent MRI studies and the HASTE technique proposed increased susceptibility to artifacts. Results yielded a statistically significant difference between the distortion rating for six of eight anatomic sites and three of eight VP variables, with the HASTE technique yielding images with less severe metal artifact and distortion. There are similarities between the distortion rating between the two techniques. For example, the anterior nasal spine and the posterior nasal spine presented with moderate or severe distortion for both imaging techniques. As a result, four of the VP variables involving these two sites were unable to be measured. The last VP variable, sagittal angle, required minimal or no distortion in the three-dimensional images to be successfully measured, and is discussed in the section below.

Although the HASTE imaging technique does not remove all susceptibility to metal artifact of orthodontic appliances, it is likely that the more frequent refocusing by radiofrequency and gradient echoes resulted significantly less blurring of VP anatomic sites of interest. Both imaging techniques are T2-weighted techniques, which result in images that emphasize fat tissue and water, compared to T1-weighted techniques which emphasize the fat tissue. The present study is focused on visualizing the LVP muscle and surrounding tissue, therefore, T2-weighted techniques were selected since muscle tissue is composed of over 80% water and result in muscles appearing brighter and more distinct (Perry et al., 2022).

MRI Scan Type

Past literature utilizing MRI for evaluation of the VP mechanism for speech has emphasized the comparison of eight main VP variables (Perry et al., 2014; Kotlarek et al., 2020; Perry et al., 2018; Haenssler, Fang, & Perry, 2020; Perry, Kuehn, & Sutton, 2014; Perry, Kuehn, & Sutton, 2013; Perry et al., 2018; Perry et al., 2017). Six of the eight VP variables can be measured using a two-dimensional image or three-dimensional image, four measured in the mid-sagittal plane and two measured in the oblique coronal plane. Two of VP variables, effective velar length and sagittal angle, requires acquisition of a three-dimensional image, as these variables require visualization of the oblique coronal plane of the levator muscle overlayed on the mid-sagittal image (Figure 5.3). Results of the present study yielded a statistically significant difference between the distortion rating for seven of eight anatomic sites and three of eight VP variables, with the 2D scans yielding images with less severe metal artifact and distortion.

The 3D scan utilizes a SPACE (sampling perfection with application optimized contrasts using different flip angle evolution), obtains a total of 176-192 slices, and requires an acquisition

time of 4-5 minutes (Perry, Sutton, Kuehn, & Gamage, 2014). The 2D scans require decreased TR and TE, obtains a total of 3-4 slices, and requires an acquisition time of 6-8 seconds. The 3D scan is beneficial because it allows the use of captured data off-line to be resampled from an infinite number of viewpoints (Bae et al., 2011). On the other hand, the 2D scan is beneficial because it allows the capturing of images during sustained phonation, as the image is obtained in a shorter time frame (6-8 seconds) compared to the 3D scan (4-5 minutes). A study by Perry et al. (2022) comparing 3D and 2D scans of adults without orthodontic appliances found that raters rated 3D scans over 2D scans for identifying velopharyngeal landmarks. However, the reliability of the raters' measures did not differ between 3D and 2D scans and authors recommended that a careful review of resources at the clinical site is critical to determine whether to use 2D or 3D scanning methods (Perry et al., 2022).

When considering an MRI of an individual with orthodontic appliance, the present study suggests that 2D scans are preferred over 3D scans. It is likely that the longer exposure to the magnetic field, due to increased acquisition time, leads to increased metal artifact (Jungmann et al., 2017; Toms et al., 2010; Ariyanayagam et al., 2015). The difference between 2D and 3D scans also suggest that as the acquisition time increases, the severity of metal artifact increases as well (Figure 4.3). Further exploration is needed to determine parameters for a 3D scan that decreases the acquisition time, but still obtaining the number of images needed for data resampling and measurement of VP variables such as effective velar length and sagittal angle.

Figure 5.3

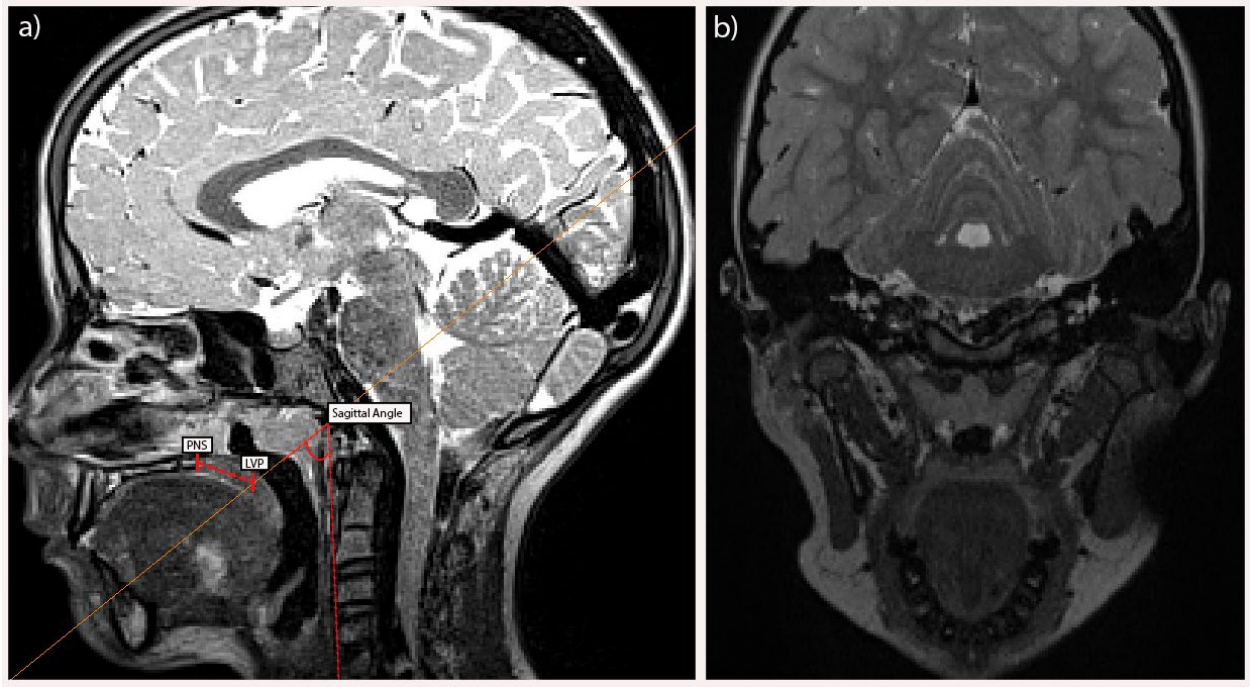

(a) MR image in the sagittal plane with the oblique coronal plane where the LVP muscle can be visualized. The orange diagonal line represents the plane in which the LVP muscle intersects the velum for measurement of the sagittal angle and the effective velar length (PNS to LVP). (b) MR image in the oblique coronal plane where the LVP muscle can be visualized.

Clinical Implications

The present study provides insights into the influence of orthodontic appliances on VP MRI. Some appliances such as hyrax palatal expanders and braces with stainless steel brackets are recommended for a VP MRI, while class II corrector springs are not recommended. The HASTE MRI sequence with 2D imaging techniques should be utilized, while FSE and 3D imaging techniques are not recommended. VP MRI of participants with orthodontic appliances is recommended for clinical cases when information about the LVP muscle length, LVP origin distance, and/or distance from velar knee to posterior pharyngeal wall needs to be obtained. Other forms of imaging, such as lateral cephalogram, should be utilized for this population to determine hard palate length, velar length, pharyngeal depth, and effective velar length. The presence of wire spring coils and molar bands are likely to not to interfere with the MRI evaluation.

The decision to recommend for a VP MRI evaluation or not should be determined by the craniofacial team. A decision tree and guidebook were created as a result of data from this study (Appendix A & B) and could be utilized when considering a referral for an MRI evaluation. The VP variables of interest and the MRI protocol is outlined specifically for each appliance type.

Communication and involvement with the orthodontist are critical to obtain information about the type of orthodontic appliance in place and the treatment plan. It is possible that between the time the MRI is scheduled and the time of the MRI evaluation, there has been a change in the patient's orthodontic appliance. While every patient is unique, most patients undergo a similar orthodontic treatment plan, beginning with the placement of a palatal expander followed by bonding of wires and brackets. For patients with more severe malocclusions, additional appliances such as the class II corrector springs, may be worn for a select period.

Clinicians should also obtain information about patient's dental history. Due to occasional delays in scheduling a VP MRI or obtaining insurance verification for the VP MRI evaluation, it is recommended that clinicians also obtain information about patient's dental history and complete an oral exam on the day of the MRI evaluation to screen for any new or unreported dental/orthodontic appliances that could potentially interfere with the VP MRI.

Lastly, one difficulty with MRI evaluation of individuals with orthodontic appliances may be obtaining insurance authorization. The present study provides details about which variables and anatomic sites are visible for each appliance type. Results from this study can be used to provide validity required by insurance companies to show the successful visualization of the LVP muscle in the oblique coronal plane for most orthodontic appliances. However, information from routine dental lateral cephalograms may be needed to obtain information in the mid-sagittal plane.

Limitations & Future Directions

This study was limited by testing only five different orthodontic appliances. Future studies should include the study of artifact by even more appliances such as ceramic and titanium brackets, quad helix palatal expander, maxillary advancement plates and screws, and embedded retainer wires. This study was limited by uneven group sizes, with group sizes varying from 1 to 8 participants. More participants with the Hyrax palatal expander and class II corrector springs should be recruited for future studies. In addition, future studies should explore different parameters of a 3D scan that decreases the acquisition time, but still obtaining the number of images needed for segmentation of the LVP muscle for measurement of VP variables such as effective velar length and sagittal angle. Different MRI scanners also have programs that can be

purchased, such as the metal artifact reduction sequences (MARS) design and software for Siemens MRI scanners, which can automatically adjust for metal artifacts (Ariyanayagam, Malcolm, & Toms, 2015). The use of such software and programs was not used in the present study and can be explored in future studies.

REFERENCES

Abbaszadeh, K., Heffez, L. B., & Mafee, M. F. (2000). Effect of interference of metallic objects on interpretation of T1-weighted magnetic resonance images in the maxillofacial region. *Oral Surgery, Oral Medicine, Oral Pathology, Oral Radiology, and Endodontology*, 89(6), 759-765.

Ahn, A. N., Monti, R. J., & Biewener, A. A. (2003). In vivo and in vitro heterogeneity of segment length changes in the semimembranosus muscle of the toad. *The Journal of physiology*, 549(3), 877-888.

Akcam, M. O., Evirgen, S., Uslu, O., & Memikoğlu, U. T. (2010). Dental anomalies in individuals with cleft lip and/or palate. *The European Journal of Orthodontics*, 32(2), 207-213.

Alaluusua, S., Turunen, L., Saarikko, A., Geneid, A., Leikola, J., & Heliövaara, A. (2019). The effects of Le Fort I osteotomy on velopharyngeal function in cleft patients. *Journal of Cranio-Maxillofacial Surgery*, 47(2), 239-244.

American Orthodontics. (2021, March 4). PowerScope™ 2 class II Corrector. Retrieved November 11, 2022, from https://www.americanortho.com/products/fixed-and-functional/powerscope-class-ii-corrector/

Anagnostara, A., Stoeckli, S., Weber, O. M., & Kollias, S. S. (2001). Evaluation of the anatomical and functional properties of deglutition with various kinetic high-speed MRI sequences. *Journal of Magnetic Resonance Imaging: An Official Journal of the International Society for Magnetic Resonance in Medicine*, 14(2), 194-199.

Angle, E. H. (1899). Classification of malocclusion. *Dental Cosmos,* 41: 248–64.

Arici, S., & Regan, D. (1997). Alternatives to ceramic brackets: the tensile bond strengths of two aesthetic brackets compared ex vivo with stainless steel foil-mesh bracket bases. *British journal of orthodontics*, 24(2), 133-137.

Ariyanayagam, T., Malcolm, P. N., & Toms, A. P. (2015, September). Advances in metal artifact reduction techniques for periprosthetic soft tissue imaging. *Seminars in musculoskeletal radiology,* 19(4), 328-334. Thieme Medical Publishers.

Asakawa, D. S., Blemker, S. S., Gold, G. E., & Delp, S. L. (2002). In vivo motion of the rectus femoris muscle after tendon transfer surgery. *Journal of biomechanics*, 35(8), 1029-1037.

Asano, S., Kaneda, T., Fukuda, T., Makiyama, Y., Hirota, H., Saitoh, K., ... & Kasai, K. (2016). Influence of metal artifact by orthodontic appliances on brain MRI. *International Journal of Oral-Medical Sciences*, 14(4), 74-81.

Bazakidou, E., Nanda, R. S., Duncanson Jr, M. G., Sinha, P., & of Oklahoma, F. T. U. (1997). Evaluation of frictional resistance in esthetic brackets. *American Journal of Orthodontics and Dentofacial Orthopedics*, 112(2), 138-144.

Beau A, Bossard D, Gebeile-Chauty S: Magnetic resonance imaging artefacts and fixed orthodontic attachments. *Eur J Orthod*, 37: 105-110, 2015.

Beer, A. J., Hellerhoff, P., Zimmermann, A., Mady, K., Sader, R., Rummeny, E. J., & Hannig, C. (2004). Dynamic near-real-time magnetic resonance imaging for analyzing the velopharyngeal closure in comparison with videofluoroscopy. *Journal of Magnetic Resonance Imaging: An Official Journal of the International Society for Magnetic Resonance in Medicine*, 20(5), 791-797.

Bell, W. H., Buche, W. A., Kennedy, J. W., & Ampil, J. P. (1977). Surgical correction of the atrophic alveolar ridge: A preliminary report on a new concept of treatment. *Oral Surgery, Oral Medicine, Oral Pathology*, 43(4), 485-498.

Bell-Berti, F. (1976). An electromyographic study of velopharyngeal function in speech. *Journal of Speech and Hearing Research*, 19(2), 225-240.

Beuf, O., Lissac, M., Crémillieux, Y., & Briguet, A. (1994). Correlation between magnetic resonance imaging disturbances and the magnetic susceptibility of dental materials. *Dental Materials*, 10(4), 265-268.

Bhatia, S., Bocca, A., Jones, J., & Sugar, A. W. (2016). Le Fort I advancement osteotomies of 1 cm or more. How safe or stable?. *British Journal of Oral and Maxillofacial Surgery*, 54(3), 346-350.

Bishara, S. E., Ortho, D., Chu, G. W., & Jakobsen, J. R. (1988). Stability of the LeFort I one-piece maxillary osteotomy. *American Journal of Orthodontics and Dentofacial Orthopedics*, 94(3), 184-200.

Bjork, A. (1951). The significance of growth changes in facial pattern and their relationship to changes in occlusion. *J Dent Res*, 71, 197-208.

Björk, A. (1963). Variations in the growth pattern of the human mandible: longitudinal radiographic study by the implant method. *Journal of Dental Research*, 42(1), 400-411.

Bjork, A., & Skieller, V. (1972). Facial development and tooth eruption: an implant study at the age of puberty. *American journal of orthodontics*, 62(4), 339-383.

Blemker, S. S., Pinsky, P. M., & Delp, S. L. (2005). A 3D model of muscle reveals the causes of nonuniform strains in the biceps brachii. *Journal of biomechanics*, 38(4), 657-665.

Böhn, A. (1963). Dental anomalies in harelip and cleft palate. *Acta Odontologica Scandinavica*, 21, 1-109.

Bongaarts, C. A., van't Hof, M. A., Prahl-Andersen, B., & Kuijpers-Jagtman, A. M. (2008). Identification of cephalometric landmarks in unilateral cleft lip and palate patients: are there alternatives for point A, ANS, and PNS?. *The Cleft palate-craniofacial journal*, 45(1), 81-86.

Boorman, J. G., & Sommerlad, B. C. (1985). Levator palati and palatal dimples: their anatomy, relationship and clinical significance. *British journal of plastic surgery*, 38(3), 326-332.

British Standards Institute. (1983) Glossary of Dental Terms. British Standards Institute.

Broadbent, B. H., Broadbent, B. H., & Golden, W. H. (1975). Bolton standards of dentofacial developmental growth. St. Louis: Mosby.

Broadwell, K. R., & Perry, J. L. (2015). Aerodynamic speech characteristics in upright and supine positions. Contemporary Issues in Communication Science and Disorders, 42(Fall), 173-181.

Buchanan, E. P., & Hyman, C. H. (2013). LeFort I osteotomy. *Seminars in plastic surgery*, 27(3), 149-154.

Burkey, P.S. (2017). Parts of Braces [Web page]. Retrieved from https://burkeyortho.com/parts-of-braces.

Calnan, J. (1961). The mobility of the soft palate: A radiological and statistical study. *British Journal of Plastic Surgery*, 14, 33-38.

Carlotti, A. E., & Schendel, S. A. (1987). An analysis of factors influencing stability of surgical advancement of the maxilla by the Le Fort I osteotomy. *Journal of oral and maxillofacial surgery*, 45(11), 924-928.

Chaimanee, P., Suzuki, B., & Suzuki, E. Y. (2011). “Safe zones” for miniscrew implant placement in different dentoskeletal patterns. *The Angle Orthodontist*, 81(3), 397-403.

Chanchareonsook, N., Whitehill, T. L., & Samman, N. (2007). Speech outcome and velopharyngeal function in cleft palate: comparison of Le Fort I maxillary osteotomy and distraction osteogenesis—early results. *The Cleft palate-craniofacial journal*, 44(1), 23-32.

Cheung, L. K., Chua, H. D. P., & Hägg, M. B. (2006). Cleft maxillary distraction versus orthognathic surgery: clinical morbidities and surgical relapse. *Plastic and reconstructive surgery*, 118(4), 996-1008.

Chua, H. D. P., Hägg, M. B., & Cheung, L. K. (2010). Cleft maxillary distraction versus orthognathic surgery—which one is more stable in 5 years?. *Oral Surgery, Oral Medicine, Oral Pathology, Oral Radiology, and Endodontology*, 109(6), 803-814.

Chua, H. D. P., Whitehill, T. L., Samman, N., & Cheung, L. K. (2010). Maxillary distraction versus orthognathic surgery in cleft lip and palate patients: effects on speech and velopharyngeal function. *International journal of oral and maxillofacial surgery*, 39(7), 633-640.

Cohen, M.S. & Mitchell, D.G. (2004). MRI principles (2nd ed.). Saunders.

Converse, J. M., & Horowitz, S. L. (1969). The surgical-orthodontic approach to the treatment of dentofacial deformities. *American journal of orthodontics*, 55(3), 217-243.

Creekmore, T. D. (1967). Inhibition or stimulation of the vertical growth of the facial complex, its significance to treatment. *The Angle Orthodontist*, 37(4), 285-297.

Creekmore, T. D., & Kunik, R. L. (1993). Straight wire: the next generation. *American Journal of Orthodontics and Dentofacial Orthopedics*, 104(1), 8-20.

Dahllof, G., Ussisoo-Joandi, R., Ideberg, M., & Modeer, T. (1989). Caries, gingivitis, and dental abnormalities in preschool children with cleft lip and/or palate. *Cleft palate J*, 26(3), 233-7.

Dalston, R. M., & Vig, P. S. (1984). Effects of orthognathic surgery on speech: a prospective study. *American journal of orthodontics*, 86(4), 291-298.

de Almeida, A. M., Ozawa, T. O., Alves, A. C. D. M., Janson, G., Lauris, J. R. P., Ioshida, M. S. Y., & Garib, D. G. (2017). Slow versus rapid maxillary expansion in bilateral cleft lip and palate: a CBCT randomized clinical trial. *Clinical oral investigations*, 21(5), 1789-1799.

de Haan, I. F., Ciesielski, R., Nitsche, T., & Koos, B. (2013). Evaluation of relapse after orthodontic therapy combined with orthognathic surgery in the treatment of skeletal class III. *Journal of Orofacial Orthopedics*, 74(5), 362-369.

De Serres, L. M., Deleyiannis, F. W. B., Eblen, L. E., Gruss, J. S., Richardson, M. A., & Sie, K. C. (1999). Results with sphincter pharyngoplasty and pharyngeal flap. *International journal of pediatric otorhinolaryngology*, 48(1), 17-25.

Delaire, J. (1971). Architectural and structural teleradiographic analysis of the face. *L'Orthodontie francaise*, 42, 411-427.

Delaire, J. (1978). Architectural and structural analysis (lateral view). *Rev Stomatol Chir Maxillofac*, 79(1), 1-33.

Delaire, J., Schendel, S. A., & Tulasne, J. F. (1981). An architectural and structural craniofacial analysis: a new lateral cephalometric analysis. *Oral Surgery, Oral Medicine, Oral Pathology*, 52(3), 226-238.

Dempsey, M. F., & Condon, B. (2001). Thermal injuries associated with MRI. *Clinical radiology*, 56(6), 457-465.

Dewinter, G., Quirynen, M., Heidbüchel, K., Verdonck, A., Willems, G., & Carels, C. (2003). Dental abnormalities, bone graft quality, and periodontal conditions in patients with unilateral cleft lip and palate at different phases of orthodontic treatment. *The Cleft Palate-Craniofacial Journal*, 40(4), 343-350.

DiBiase, A. (2002). The timing of orthodontic treatment. Dental Update, 29(9), 434-441.

Donnelly, L. F. (2005). Obstructive sleep apnea in pediatric patients: evaluation with cine MR sleep studies. *Radiology*, 236(3), 768-778.

Dowling, P. A., Espeland, L., Sandvik, L., Mobarak, K. A., & Hogevold, H. E. (2005). LeFort I maxillary advancement: 3-year stability and risk factors for relapse. *American journal of orthodontics and dentofacial orthopedics*, 128(5), 560-567.

Drost, M. R., Maenhout, M., Willems, P. J. B., Oomens, C. W. J., Baaijens, F. P. T., & Hesselink, M. K. C. (2003). Spatial and temporal heterogeneity of superficial muscle strain during in situ fixed-end contractions. *Journal of biomechanics*, 36(7), 1055-1063.

Eggers, G., Rieker, M., Kress, B., Fiebach, J., Dickhaus, H., & Hassfeld, S. (2005). Artefacts in magnetic resonance imaging caused by dental material. *Magnetic Resonance Materials in Physics, Biology and Medicine*, 18(2), 103-111.

Elison JM, Leggitt VL, Thomson M, Oyoyo U, Wycliffe ND: Influence of common orthodontic appliances on the diagnostic quality of cranial magnetic resonance images. *Am J Orthod Dentofacial Orthop*, 134: 563-572, 2008.

Engwall, O. (2003). A revisit to the application of MRI to the analysis of speech production-testing our assump[1]tions. Proceedings of the 6th International Seminar on Speech Production, 43–48.

Eser, C., Gencel, E., Gokdogan, M., Kesiktaş, E., & Yavuz, O. S. M. A. N. (2015). Comparison of autologous and heterologous bone graft stability effects for filling maxillary bone gap after Le Fort I osteotomy. *Advances in Clinical and Experimental Medicine*, 24(2).

Eskenazi, L. B., & Schendel, S. A. (1992). An analysis of Le Fort I maxillary advancement in cleft lip and palate patients. *Plastic and reconstructive surgery*, 90, 779-779.

Fache, J. S., Price, C., Hawbolt, E. B., & Li, D. K. (1987). MR imaging artifacts produced by dental materials. *American journal of neuroradiology*, 8(5), 837-840.

Fahradyan, A., Wolfswinkel, E. M., Clarke, N., Park, S., Tsuha, M., Urata, M. M., ... & Yamashita, D. D. R. (2018). Impact of the distance of maxillary advancement on horizontal relapse after orthognathic surgery. *The Cleft Palate-Craniofacial Journal*, 55(4), 546-553.

Fiala, T. G., Paige, K. T., Davis, T. L., Campbell, T. A., Rosen, B. R., & Yaremchuk, M. J. (1994). Comparison of artifact from craniomaxillofacial internal fixation devices: magnetic resonance imaging. *Plastic and reconstructive surgery*, 93(4), 725-731.

Figueroa, A. A., Polley, J. W., Friede, H., & Ko, E. W. (2004). Long-term skeletal stability after maxillary advancement with distraction osteogenesis using a rigid external distraction device in cleft maxillary deformities. *Plastic and reconstructive surgery*, 114(6), 1382-1392.

Filip, C., Impieri, D., Aagenæs, I., Breugem, C., Høgevold, H. E., Særvold, T., ... & Abrahamsen, T. G. (2018). Adults with 22q11. 2 deletion syndrome have a different velopharyngeal anatomy with predisposition to velopharyngeal insufficiency. *Journal of Plastic, Reconstructive & Aesthetic Surgery*, 71(4), 524-536.

Fleck, R. J., Shott, S. R., Mahmoud, M., Ishman, S. L., Amin, R. S., & Donnelly, L. F. (2018). Magnetic resonance imaging of obstructive sleep apnea in children. *Pediatric radiology,* 48(9), 1223-1233.

Freitas, J. A. D. S., Garib, D. G., Oliveira, M., Lauris, R. D. C. M. C., Almeida, A. L. P. F. D., Neves, L. T., ... & Pinto, J. H. N. (2012). Rehabilitative treatment of cleft lip and palate: experience of the Hospital for Rehabilitation of Craniofacial Anomalies-USP (HRAC-USP)-Part 2: Pediatric Dentistry and Orthodontics. *Journal of Applied Oral Science*, 20, 268-281.

Gilbert, R. J., Daftary, S., Campbell, T. A., & Weisskoff, R. M. (1998). Patterns of lingual tissue deformation associated with bolus containment and propulsion during deglutition as determined by echo-planar MRI. *Journal of Magnetic Resonance Imaging*, 8(3), 554-560.

Gohilot, A., Pradhan, T., & Keluskar, K. M. (2014). Cephalometric evaluation of adenoids, upper airway, maxilla, velum length, need ratio for determining velopharyngeal incompetency in subjects with unilateral cleft lip and palate. *Journal of Indian Society of Pedodontics and Preventive Dentistry*, 32(4), 297.

Gomes, K. U., Martins, W. D. B., & Ribas, M. D. O. (2013). Horizontal and vertical maxillary osteotomy stability, in cleft lip and palate patients, using allogeneic bone graft. *Dental press journal of orthodontics*, 18, 84-90.

Good, P. M., Mulliken, J. B., & Padwa, B. L. (2007). Frequency of Le Fort I osteotomy after repaired cleft lip and palate or cleft palate. *The Cleft palate-craniofacial journal*, 44(4), 396-401.

Gordon, A. M., Huxley, A. F., & Julian, F. J. (1966). The variation in isometric tension with sarcomere length in vertebrate muscle fibres. *The Journal of physiology*, 184(1), 170-192.

Gray, C. F., Redpath, T. W., & Smith, F. W. (1996). Pre-surgical dental implant assessment by magnetic resonance imaging. *The Journal of oral implantology*, 22(2), 147-153.

Gray, C. F., Redpath, T. W., Smith, F. W., & Staff, R. T. (2003). Advanced imaging: magnetic resonance imaging in implant dentistry: a review. *Clinical oral implants research*, 14(1), 18-27.

Haapanen, M. L., Kalland, M., Heliövaara, A., Hukki, J., & Ranta, R. (1997). Velopharyngeal function in cleft patients undergoing maxillary advancement. *Folia phoniatrica et logopaedica*, 49(1), 42-47.

Haenssler, A. E., Baylis, A., Perry, J. L., Kollara, L., Fang, X., & Kirschner, R. (2020). Impact of cranial base abnormalities on cerebellar volume and the velopharynx in 22q11. 2 deletion syndrome. *The Cleft Palate-Craniofacial Journal*, 57(4), 412-419.

Haenssler, A. E., Fang, X., & Perry, J. L. (2020). Effective velopharyngeal ratio: A more clinically relevant measure of velopharyngeal function. *Journal of Speech, Language, and Hearing Research*, 63(11), 3586-3593.

Haenssler, A. E., Perry, J. L., Mann, S. A., & Mann, R. J. (2021). An MRI Case Study: The Anatomic Cleft Restoration Concept Utilizing Buccal Flaps in a Primary Palatoplasty. *FACE,* 2(2), 174-178.

Hardy, D. K., Cubas, Y. P., & Orellana, M. F. (2012). Prevalence of angle class III malocclusion: A systematic review and meta-analysis.

Hassan, T., Naini, F. B., & Gill, D. S. (2007). The effects of orthognathic surgery on speech: a review. *Journal of oral and maxillofacial surgery*, 65(12), 2536-2543.

Heasman, P. (2009). Master Dentistry Volume 2. Churchill Livingstone.

Hellman, M. (1933). Growth of the Face and Occlusion of the Teeth in Relation to Orthodontic Treatment. *International Journal of Orthodontia and Dentistry for Children*, 19(11), 1116-1147.

Hinshaw Jr, D. B., Holshouser, B. A., Engstrom, H. I., Tjan, A. H., Christiansen, E. L., & Catelli, W. F. (1988). Dental material artifacts on MR images. *Radiology*, 166(3), 777-779.

Hirano, A., & Suzuki, H. (2001). Factors related to relapse after Le Fort I maxillary advancement osteotomy in patients with cleft lip and palate. *The Cleft palate-craniofacial journal*, 38(1), 1-10.

Hochban, W., Ganß, C., & Austermann, K. H. (1993). Long-term results after maxillary advancement in patients with clefts. *The Cleft palate-craniofacial journal*, 30(2), 237-243.

Hong, M., & Baek, S. H. (2018). Differences in the alignment pattern of the maxillary dental arch following fixed orthodontic treatment in patients with bilateral cleft lip and palate:

anteroposterior-collapsed arch versus transverse-collapsed arch. *Journal of Craniofacial Surgery*, 29(2), 440-444.

Hotz, M. & Gnoinski, W. (1976) Comprehensive care of cleft lip and palate children at Zurich University: a preliminary report. *Am J Orthod*, 70:481-504.

Houston, W. J., James, D. R., Jones, E., & Kavvadia, S. (1989). Le Fort I maxillary osteotomies in cleft palate cases: surgical changes and stability. *Journal of Cranio-Maxillofacial Surgery*, 17(1), 9-15.

Hubálková, H., Hora, K., Seidl, Z., & Krásenský, J. (2002). Dental materials and magnetic resonance imaging. *The European journal of prosthodontics and restorative dentistry*, 10(3), 125-130.

Hubálková, H., La Serna, P., Linetskiy, I., & Dostálová, T. J. (2006). Dental alloys and magnetic resonance imaging. *International dental journal*, 56(3), 135-141.

Hultgren, B. W., Isaacson, R. J., Erdman, A. G., Worms, F. W., & Rekow, E. D. (1980). Growth contributions to Class II corrections based on models of mandibular morphology. *American journal of orthodontics*, 78(3), 310-320.

Iannetti, G., Cascone, P., Saltarel, A., & Ettaro, G. (2004). Le Fort I in cleft patients: 20 years' experience. *Journal of Craniofacial Surgery*, 15(4), 662-669.

Iannetti, G., Chimenti, C., & Di Paolo, C. (1987). Five-year follow-up of Le Fort I osteotomies. *Journal of Cranio-Maxillofacial Surgery*, 15, 238-243.

Impieri, D., Tønseth, K. A., Hide, Ø., Brinck, E. L., Høgevold, H. E., & Filip, C. (2018). Impact of orthognathic surgery on velopharyngeal function by evaluating speech and cephalometric radiographs. *Journal of Plastic, Reconstructive & Aesthetic Surgery*, 71(12), 1786-1795.

Inman, D. S., Thomas, P., Hodgkinson, P. D., & Reid, C. A. (2005). Oro-nasal fistula development and velopharyngeal insufficiency following primary cleft palate surgery—an audit of 148 children born between 1985 and 1997. *British journal of plastic surgery*, 58(8), 1051-1054.reconstructive surgery, 112(7), 1755-1761.

Innovative Orthodontic Centers (2022). Parts of braces [Web page]. Retrieved from https://www.innovativeorthocenters.com/parts-of-braces/.

Inouye, J. M., Perry, J. L., Lin, K. Y., & Blemker, S. S. (2015). A computational model quantifies the effect of anatomical variability on velopharyngeal function. *Journal of speech, language, and hearing research*, 58(4), 1119-1133.

Inouye, S. Y. (1957). A serial study of the soft tissue profile of individuals with excellent occlusions (Doctoral dissertation, University of Washington, Seattle).

Isaacson, J. R., Isaacson, R. J., Speidel, T. M., & Worms, F. W. (1971). Extreme variation in vertical facial growth and associated variation in skeletal and dental relations. *Angle orthod*, 41(3), 219-29.

Isaacson, R. J., Zapfel, R. J., Worms, F. W., & Erdman, A. G. (1977). Effects of rotational jaw growth on the occlusion and profile. *American journal of orthodontics*, 72(3), 276-286.

Isaacson, R. J., Zapfel, R. J., Worms, F. W., Bevis, R. R., & Speidel, T. M. (1977). Some effects of mandibular growth on the dental occlusion and profile. *Angle orthodontist*, 47(2), 97-106.

Isaacson, R., Erdman, A., & Hultgren, B. (1981). Facial and dental effects of mandibular rotation. Craniofacial Biology Craniofacial Growth Series, (10).

Johnston, C., Burden, D., Kennedy, D., Harradine, N., & Stevenson, M. (2006). Class III surgical-orthodontic treatment: a cephalometric study. *American journal of orthodontics and dentofacial orthopedics,* 130(3), 300-309.

Jordan, R. E., Kraus, B. S., & Neptune, C. M. (1966). Dental abnormalities associated with cleft lip and/or palate. *The Cleft Palate Journal*, 3, 22-55.

Jungmann, P. M., Agten, C. A., Pfirrmann, C. W., & Sutter, R. (2017). Advances in MRI around metal. *Journal of magnetic resonance imaging*, 46(4), 972-991.

Kemper, J., Priest, A. N., Schulze, D., Kahl-Nieke, B., Adam, G., & Klocke, A. (2007). Orthodontic springs and auxiliary appliances: assessment of magnetic field interactions associated with 1.5 T and 3 T magnetic resonance systems. *European radiology*, 17(2), 533-540.

Kiely, K. D., Wendfeldt, K. S., Johnson, B. E., Haskell, B. S., & Edwards, R. C. (2006). One-year postoperative stability of LeFort I osteotomies with biodegradable fixation: a retrospective analysis of skeletal relapse. *American journal of orthodontics and dentofacial orthopedics,* 130(3), 310-316.

Kim, Y. C. (2018). Fast upper airway magnetic resonance imaging for assessment of speech production and sleep apnea. *Precision and Future Medicine*, 2(4), 131-148.

Klinke, T., Daboul, A., Maron, J., Gredes, T., Puls, R., Jaghsi, A., & Biffar, R. (2012). Artifacts in magnetic resonance imaging and computed tomography caused by dental materials. PLoS One, 7(2), e31766.

Klocke, A., Kemper, J., Schulze, D., Adam, G., & Kahl-Nieke, B. (2005). Magnetic field interactions of orthodontic wires during magnetic resonance imaging (MRI) at 1.5 Tesla. *Journal of Orofacial Orthopedics*, 66(4), 279-287.

Kollara, L., & Perry, J. L. (2014). Effects of gravity on the velopharyngeal structures in children using upright magnetic resonance imaging. *The Cleft Palate-Craniofacial Journal*, 51(6), 669-676.

Kollara, L., Baylis, A. L., Kirschner, R. E., Bates, D. G., Smith, M., Fang, X., & Perry, J. L. (2019). Velopharyngeal structural and muscle variations in children with 22q11. 2 deletion syndrome: an unsedated MRI study. *The Cleft Palate-Craniofacial Journal*, 56(9), 1139-1148.

Kollara, L., Perry, J. L., & Hudson, S. (2016). Racial variations in velopharyngeal and craniometric morphology in children: an imaging study. *Journal of Speech, Language, and Hearing Research*, 59(1), 27-38.

Kollara, L., Perry, J. L., Kirschner, R. E., Fang, X., & Baylis, A. L. (2022). Assessment of the Velopharyngeal Mechanism at Rest and During Speech in Children With 22q11. 2DS: A Cross-Sectional Study. *The Cleft Palate-Craniofacial Journal*, 10556656221100674.

Kollara, L., Schenck, G., Jaskolka, M., & Perry, J. L. (2017). Examining a new method to studying velopharyngeal structures in a child with 22q11. 2 deletion syndrome. *Journal of Speech, Language, and Hearing Research*, 60(4), 892-896.

Kotlarek, K. J., Haenssler, A. E., Hildebrand, K. E., & Perry, J. L. (2019). Morphological variation of the velum in children and adults using magnetic resonance imaging. *Imaging science in dentistry*, 49(2), 153-158.

Kotlarek, K. J., Pelland, C. M., Blemker, S. S., Jaskolka, M. S., Fang, X., & Perry, J. L. (2020). Asymmetry and positioning of the levator veli palatini muscle in children with repaired cleft palate. *Journal of Speech, Language, and Hearing Research*, 63(5), 1317-1325.

Kotlarek, K. J., Perry, J. L., & Jaskolka, M. S. (2022). What is the fate of the pedicled buccal fat pad flap when used during primary palatoplasty?. *Journal of Craniofacial Surgery*, 33(2), e173-e175.

Kotlarek, K. J., Sitzman, T. J., Williams, J. L., & Perry, J. L. (2021). Nonsedated Magnetic Resonance Imaging for Visualization of the Velopharynx in the Pediatric Population. *The Cleft Palate-Craniofacial Journal,* 10556656211057361.

Krogman, W. M., Mazaheri, M., Harding, R. L., Ishiguro, K., Bariana, G., Meier, J., ... & Ross, P. (1975). A longitudinal study of the craniofacial growth pattern in children with clefts as compared to normal, birth to six years. *The Cleft palate journal*, 12(1), 59-84.

Küchler, E. C., da Motta, L. G., Vieira, A. R., & Granjeiro, J. M. (2011). Side of dental anomalies and taurodontism as potential clinical markers for cleft subphenotypes. *The Cleft palate-craniofacial journal*, 48(1), 103-108.

Kuehn, D. P., Ettema, S. L., Goldwasser, M. S., & Barkmeier, J. C. (2004). Magnetic resonance imaging of the levator veli palatini muscle before and after primary palatoplasty. *The Cleft Palate-Craniofacial Journal*, 41(6), 584-592.

Kuehn, D.P. (1979). Velopharyngeal anatomy and physiology. *Ear Nose Throat Journal*, 58(7), 316-321.

Kusy, R. P., & Whitley, J. Q. (1990). Effects of surface roughness on the coefficients of friction in model orthodontic systems. *Journal of Biomechanics*, 23(9), 913-925.

Lande, M. J. (1952). Growth behavior of the human bony facial profile as revealed by serial cephalometric roentgenology. *The Angle Orthodontist*, 22(2), 78-90.

Lavergne, J., & Gasson, N. (1976). A metal implant study of mandibular rotation. *The Angle orthodontist*, 46(2), 144-150.

Lavergne, J., & Gasson, N. (1978). The influence of jaw rotation on the morphogenesis of malocclusion. *American journal of orthodontics,* 73(6), 658-666.

Letra, A., Menezes, R., Granjeiro, J. M., & Vieira, A. R. (2007). Defining subphenotypes for oral clefts based on dental development. *Journal of dental research*, 86(10), 986-991.

Lipson, A. H., Yuille, D., Angel, M., Thompson, P. G., Vandervoord, J. G., & Beckenham, E. J. (1991). Velocardiofacial (Shprintzen) syndrome: an important syndrome for the dysmorphologist to recognise. *Journal of Medical Genetics*, 28(9), 596-604.

Losken, A., Williams, J. K., Burstein, F. D., Malick, D., & Riski, J. E. (2003). An outcome evaluation of sphincter pharyngoplasty for the management of velopharyngeal insufficiency. *Plastic and reconstructive surgery*, 112(7), 1755-1761.

Louis, P. J., Waite, P. D., & Austin, R. B. (1993). Long-term skeletal stability after rigid fixation of Le Fort I osteotomies with advancements. *International journal of oral and maxillofacial surgery*, 22(2), 82-86.

Lu, Y., Shi, B., Zheng, Q., Xiao, W., & Li, S. (2006). Analysis of velopharyngeal morphology in adults with velopharyngeal incompetence after surgery of a cleft palate. *Annals of Plastic Surgery*, 57(1), 50-54.

Lubker, J. F., & Parris, P. J. (1970). Simultaneous measurements of intraoral pressure, force of labial contact, and labial electromyographic activity during production of the stop consonant cognates /p/ and /b/. *The Journal of the Acoustical Society of America*, 47(2B), 625-633.

Machos, C. C. (1996, September). Orthodontic treatment for the cleft palate patient. *Seminars in orthodontics,* 2(3), 197-204. WB Saunders.

Maijer, R., & Smith, D. C. (1982). Corrosion of orthodontic bracket bases. *American Journal of Orthodontics*, 81(1), 43-48.

Mann, S. A., Mann, R. J., Haenssler, A. E., & Perry, J. L. (2020). An magnetic resonance imaging case study: the anatomic palate restoration concept utilizing buccal flaps in a primary palatoplasty. *Plastic and Reconstructive Surgery–Global Open*, 8(9S), 112-113.

Manner, I., Alanen, A., Komu, M., Savunen, T., Kantonen, I., & Ekfors, T. (1996). MR imaging in the presence of small circular metallic implants: assessment of thermal injuries. *Acta Radiologica*, 37(4), 551-554.

Mason, K. N. (2017). The Effects of Gravity and Scar Contracture on Post-Surgical Tissue Changes and Speech Outcomes Following Pharyngoplasties. (Doctoral Dissertation, East Carolina University, Greenville, NC)

Mason, K. N., Pua, E., & Perry, J. L. (2018). Effect of motor-based speech intervention on articulatory placement in the treatment of a posterior nasal fricative: a preliminary MRI study on a single subject. *International Journal of Language & Communication Disorders*, 53(4), 852-863.

Mason, K. N., Riski, J. E., Williams, J. K., Jones, R. A., & Perry, J. L. (2021). Utilization of 3D MRI for the Evaluation of Sphincter Pharyngoplasty Insertion Site in Patients With Velopharyngeal Dysfunction. *The Cleft Palate-Craniofacial Journal*, 10556656211044656.

Mason, K., & Perry, J. (2017). The use of magnetic resonance imaging (MRI) for the study of the velopharynx. *Perspectives of the ASHA Special Interest Groups,* 2(5), 35-52.

Mason, R. M. (1969). Clinical relationships between adenoids and velopharyngeal competency. *The Journal of the Tennessee Speech and Hearing Association*, 14, 15-25.

McCarthy, J. G., Coccaro, P. J., & Schwartz, M. D. (1979). Velopharyngeal function following maxillary advancement. *Plastic and Reconstructive Surgery*, 64(2), 180-189.

McComb, R. W., Marrinan, E. M., Nuss, R. C., LaBrie, R. A., Mulliken, J. B., & Padwa, B. L. (2011). Predictors of velopharyngeal insufficiency after Le Fort I maxillary advancement in patients with cleft palate. *Journal of oral and maxillofacial surgery*, 69(8), 2226-2232.

McDermott, M. (2022). Different parts of orthodontic braces [Web page]. Retrieved from https://www.mcdermottortho.com/parts-of-braces/.

Menezes, R., & Vieira, A. R. (2008). Dental anomalies as part of the cleft spectrum. *The Cleft Palate-Craniofacial Journal*, 45(4), 414-419.

Mitchell, L., Littlewood, S.J., Nelson-Moon, Z.L., & Dyer, F. (2013). Introduction to Orthodontics (4th Edition). Oxford University Press.

Moon, J. B., & Kuehn, D. P. (1997). Anatomy and physiology of normal and disordered velopharyngeal function for speech. Communicative disorders related to cleft lip and palate. 4th edition. Austin: Pro-Ed, 45-7.

Moresca, R., Moro, A., Dominguez, G. C., & Vigorito, J. W. (2011). Effects of nickel-titanium and stainless steel leveling wires on the position of mandibular incisors. *Dental Press Journal of Orthodontics*, 16, 74-81.

Nakamura, N., Ogata, Y., Kunimitsu, K., Suzuki, A., Sasaguri, M., & Ohishi, M. (2003). Velopharyngeal morphology of patients with persistent velopharyngeal incompetence following repushback surgery for cleft palate. *The Cleft palate-craniofacial journal*, 40(6), 612-617.

Nohara, K., Tachimura, T., & Wada, T. (2006). Prediction of deterioration of velopharyngeal function associated with maxillary advancement using electromyography of levator veli palatini muscle. *The Cleft palate-craniofacial journal*, 43(2), 174-178.

Odegaard, J. (1970). Mandibular rotation studied with the aid of metal implants. *American journal of orthodontics*, 58(5), 448-454.

Ortiz, O., Pait, T. G., McAllister, P., & Sauter, K. (1996). Postoperative magnetic resonance imaging with titanium implants of the thoracic and lumbar spine. *Neurosurgery,* 38(4), 741-745.

Pandis, N., & Bourauel, C. P. (2010, December). Nickel-titanium (NiTi) arch wires: the clinical significance of super elasticity. *Seminars in Orthodontics,* 16(4), 249-257. WB Saunders.

Pappas, G. P., Asakawa, D. S., Delp, S. L., Zajac, F. E., & Drace, J. E. (2002). Nonuniform shortening in the biceps brachii during elbow flexion. *Journal of applied physiology*, 92(6), 2381-2389.

Patel, M. R., Klufas, R. A., Alberico, R. A., & Edelman, R. R. (1997). Half-fourier acquisition single-shot turbo spin-echo (HASTE) MR: comparison with fast spin-echo MR in diseases of the brain. *American journal of neuroradiology*, 18(9), 1635-1640.

Pereira, V. J., Sell, D., & Tuomainen, J. (2013). Effect of maxillary osteotomy on speech in cleft lip and palate: perceptual outcomes of velopharyngeal function. *International journal of language & communication disorders*, 48(6), 640-650.

Perry JL. (2011b) Variations in velopharyngeal structures between upright and supine positions using upright magnetic resonance imaging. *Cleft Palate Craniofac J*, 48(2):123-33. doi: 10.1597/09-256.

Perry, J. (2007). Magnetic Resonance Imaging and Three-Dimensional Computer Modeling of the Levator Veli Palatini Muscle Before and After Primary Palatoplasty (Doctoral dissertation, University of Illinois at Urbana-Champaign).

Perry, J. L. (2011a). Anatomy and physiology of the velopharyngeal mechanism. In Seminars in speech and language (Vol. 32, No. 02, pp. 083-092). © Thieme Medical Publishers.

Perry, J. L., & Kuehn, D. P. (2009). Magnetic resonance imaging and computer reconstruction of the velopharyngeal mechanism. *Journal of Craniofacial Surgery*, 20(8), 1739-1746.

Perry, J. L., Haenssler, A. E., Kotlarek, K. J., Chen, J. Y., Fang, X., Guo, Y., ... & Webb, M. (2022). Does the Type of MRI Sequence Influence Perceived Quality and Measurement Consistency in Investigations of the Anatomy of the Velopharynx?. *The Cleft Palate-Craniofacial Journal*, 59(6), 741-750.

Perry, J. L., Kollara, L., Sutton, B. P., Kuehn, D. P., & Fang, X. (2019). Growth effects on velopharyngeal anatomy from childhood to adulthood. *Journal of Speech, Language, and Hearing Research*, 62(3), 682-692.

Perry, J. L., Kotlarek, K. J., Sutton, B. P., Kuehn, D. P., Jaskolka, M. S., Fang, X., ... & Rauccio, F. (2018). Variations in velopharyngeal structure in adults with repaired cleft palate. *The Cleft Palate-Craniofacial Journal*, 55(10), 1409-1418.

Perry, J. L., Kuehn, D. P., & Sutton, B. P. (2013). Morphology of the levator veli palatini muscle using magnetic resonance imaging. *The Cleft Palate-Craniofacial Journal*, 50(1), 64-75.

Perry, J. L., Kuehn, D. P., Sutton, B. P., & Fang, X. (2017). Velopharyngeal structural and functional assessment of speech in young children using dynamic magnetic resonance imaging. *The Cleft Palate-Craniofacial Journal*, 54(4), 408-422.

Perry, J. L., Sutton, B. P., Kuehn, D. P., & Gamage, J. K. (2014). Using MRI for assessing velopharyngeal structures and function. *The Cleft Palate-Craniofacial Journal*, 51(4), 476-486.

Perry, J., Kuehn, D., Sutton, B., Goldwasser, M., & Jerez, A. (2010). MRI and 3D Computer Modeling of the Levator Veli Palatini Muscle Before and After Primary Palatoplasty. *The Cleft palate-craniofacial journal.*

Polley, J. W., & Figueroa, A. A. (1997). Distraction osteogenesis: its application in severe mandibular deformities in hemifacial microsomia. *The Journal of craniofacial surgery*, 8(5), 422-430.

Posnick, J. C., & Ewing, M. P. (1990). Skeletal stability after Le Fort I maxillary advancement in patients with unilateral cleft lip and palate. *Plastic and reconstructive surgery*, 85(5), 706-710.

Pöyry, M., & Ranta, R. (1985). Anomalies in the deciduous dentition outside the cleft region in children with oral clefts. Proceedings of the Finnish Dental Society. Suomen Hammaslaakariseuran Toimituksia, 81(2), 91-97.

Proffit, W. R., Phillips, C., & Turvey, T. A. (1987). Stability following superior repositioning of the maxilla by LeFort I osteotomy. *American journal of orthodontics and dentofacial orthopedics*, 92(2), 151-161.

Proffit, W. R., Turvey, T. A., & Phillips, C. (1996). Orthognathic surgery: a hierarchy of stability. *The International journal of adult orthodontics and orthognathic surgery*, 11(3), 191-204.

Pugliese, F., Palomo, J. M., Calil, L. R., de Medeiros Alves, A., Lauris, J. R. P., & Garib, D. (2020). Dental arch size and shape after maxillary expansion in bilateral complete cleft palate: A comparison of three expander designs. *The Angle Orthodontist,* 90(2), 233-238.

Rakosi, T. (1982). An atlas and manual of cephalometric radiography.

Regier, M., Kemper, J., Kaul, M. G., Feddersen, M., Adam, G., Kahl-Nieke, B., & Klocke, A. (2009). Radiofrequency-induced heating near fixed orthodontic appliances in high field MRI systems at 3.0 Tesla. *Journal of Orofacial Orthopedics*, 70(6), 485.

Ribeiro, L., Teixeira das Neves, L., Costa, B., & Ribeiro Gomide, M. (2003). Dental anomalies of the permanent lateral incisors and prevalence of hypodontia outside the cleft area in complete unilateral cleft lip and palate. *The Cleft palate-craniofacial journal*, 40(2), 172-175.

Rommel, N., Vantrappen, G., Swillen, A., Devriendt, K., Feenstra, L., & Fryns, J. P. (1999). Retrospective analysis of feeding and speech disorders in 50 patients with velo-cardio-facial syndrome. *Genetic counseling* (Geneva, Switzerland), 10(1), 71-78.

Ross, R. B. (1987). Treatment variables affecting facial growth in complete unilateral cleft lip and palate. Part 3: alveolus repair and bone grafting. *The Cleft Palate Journal*, 24(1), 33-44.

Rygh, P., & Sirinavin, I. (1982). Craniofacial morphology in six-year-old Norwegian boys with complete cleft of lip and palate. *Swedish Dental journal*. Supplement, 15, 203-213.

Sales, P. H. H., Costa, F. W. G., Cetira Filho, E. L., Silva, P. G. B., Albuquerque, A. F. M., & Leão, J. C. (2021). Effect of maxillary advancement on speech and velopharyngeal function of patients with cleft palate: Systematic Review and Meta-Analysis. *International Journal of Oral and Maxillofacial Surgery*, 50(1), 64-74.

Saltaji, H., Major, M. P., Alfakir, H., Al-Saleh, M. A., & Flores-Mir, C. (2012). Maxillary advancement with conventional orthognathic surgery in patients with cleft lip and palate: is it a stable technique?. *Journal of oral and maxillofacial surgery*, 70(12), 2859-2866.

Satoh, K., Nagata, J., Shomura, K., Wada, T., Tachimura, T., Fukuda, J., & Shiba, R. (2004). Morphological evaluation of changes in velopharyngeal function following maxillary

distraction in patients with repaired cleft palate during mixed dentition. *The Cleft palate-craniofacial journal*, 41(4), 355-363.

Satoh, K., Wada, T., Tachimura, T., & Fukuda, J. (2005). Velar ascent and morphological factors affecting velopharyngeal function in patients with cleft palate and noncleft controls: a cephalometric study. *International journal of oral and maxillofacial surgery*, 34(2), 122-126.

Savara, B. S., & Singh, I. J. (1968). Norms of size and annual increments of seven anatomical measures of maxillae in boys from three to sixteen years of age. *The Angle Orthodontist*, 38(2), 104-120.

Schenck, G. C., Perry, J. L., O'Gara, M. M., Linde, A. M., Grasseschi, M. F., Wood, R. J., ... & Fang, X. (2021). Velopharyngeal muscle morphology in children with unrepaired submucous cleft palate: An imaging study. *The Cleft Palate-Craniofacial Journal*, 58(3), 313-323.

Schendel, S. A., Oeschlaeger, M., Wolford, L. M., & Epker, B. N. (1979). Velopharyngeal anatomy and maxillary advancement. *Journal of maxillofacial surgery*, 7, 116-124.

Schroeder, D. C., & Green, L. J. (1975). Frequency of dental trait anomalies in cleft, sibling, and noncleft groups. *Journal of dental research*, 54(4), 802-807.

Schudy, F. F. (1963). Cant of the occlusal plane and axial inclinations of teeth. *The Angle Orthodontist*, 33(2), 69-82.

Schudy, F. F. (1964). Vertical growth versus anteroposterior growth as related to function and treatment. *The Angle Orthodontist,* 34(2), 75-93.

Schudy, F. F. (1965). The rotation of the mandible resulting from growth: its implications in orthodontic treatment. *The Angle Orthodontist*, 35(1), 36-50.

Schultz, K. P., Braun, T. L., Hernandez, C., Wilson, K. D., Moore, E. E., Wirthlin, J. O., ... & Monson, L. A. (2019). Speech outcomes after LeFort I advancement among cleft lip and palate patients. *Annals of plastic surgery*, 82(2), 174-179.

Schwarz, C., & Gruner, E. (1976). Logopaedic findings following advancement of the maxilla. *Journal of maxillofacial surgery*, 4, 40-55.

Scolozzi, P. (2008). Distraction osteogenesis in the management of severe maxillary hypoplasia in cleft lip and palate patients. *Journal of Craniofacial Surgery*, 19(5), 1199-1214.

Shafiei, F., Honda, E., Takahashi, H., & Sasaki, T. (2003). Artifacts from dental casting alloys in magnetic resonance imaging. *Journal of dental research*, 82(8), 602-606.

Shalish M, Dykstein N, Friedlander-Barenboim S, Ben-David E, Gomori JM, Chaushu S: Influence of common fixed retainers on the diagnostic quality of cranial magnetic resonance images. *Am J Orthod Dentofacial Orthop*, 147: 604-609, 2015.

Shapira, Y., Lubit, E., & Kuftinec, M. M. (2000). Hypodontia in children with various types of clefts. *The Angle Orthodontist,* 70(1), 16-21.

Sharma, K. (2017, January 17). Braces parts and use [Web page]. Retrieved from https://patients.dentistry.utoronto.ca/braces-parts-and-use.

Shellock, F. G. (2000). Radiofrequency energy-induced heating during MR procedures: a review. *Journal of Magnetic Resonance Imaging*, 12(1), 30-36.

Shellock, F. G., & Kanal, E. (1998). Aneurysm clips: evaluation of MR imaging artifacts at 1.5 T. *Radiology*, 209(2), 563-566.

Shprintzen, R. J. (2008). Velo-cardio-facial syndrome: 30 years of study. *Developmental disabilities research reviews*, 14(1), 3-10.

Sie, K. C., Tampakopoulou, D. A., De Serres, L. M., Grass, J. S., Eblen, L. E., & Yonick, T. (1998). Sphincter pharyngoplasty: speech outcome and complications. *The Laryngoscope*, 108(8), 1211-1217.

Sinclair, P. M., & Little, R. M. (1985). Dentofacial maturation of untreated normals. *American Journal of Orthodontics*, 88(2), 146-156.

Smatt, Y., & Ferri, J. (2005). Retrospective study of 18 patients treated by maxillomandibular advancement with adjunctive procedures for obstructive sleep apnea syndrome. *Journal of Craniofacial Surgery*, 16(5), 770-777.

Solot, C. B., Gerdes, M., Kirschner, R. E., McDonald-McGinn, D. M., Moss, E., Woodin, M., ... & Wang, P. P. (2001). Communication issues in 22q11. 2 deletion syndrome: children at risk. *Genetics in Medicine*, 3(1), 67-71.

Starčuková, J., Starčuk Jr, Z., Hubálková, H., & Linetskiy, I. (2008). Magnetic susceptibility and electrical conductivity of metallic dental materials and their impact on MR imaging artifacts. *Dental materials*, 24(6), 715-723.

Steiner, C. (1953). Cephalometrics for you and me. *Am J Orthod*, 39(10), 729-755.

Steiner, C. C. (1959). Cephalometrics in clinical practice. *The Angle Orthodontist*, 29(1), 8-29.

Steiner, C. C. (1960). The use of cephalometrics as an aid to planning and assessing orthodontic treatment: report of a case. *American journal of orthodontics*, 46(10), 721-735.

Subtelny, J. D. (1957). A cephalometric study of the growth of the soft palate. *Plastic and Reconstructive Surgery*, 19(1), 49-62.

Subtelny, J. D. (1959). A longitudinal study of soft tissue facial structures and their profile characteristics, defined in relation to underlying skeletal structures. *American Journal of Orthodontics*, 45(7), 481-507.

Suto, Y., Matsuo, T., Kato, T., Hori, I., Inoue, Y., Ogawa, S., ... & Ohta, Y. (1993). Evaluation of the pharyngeal airway in patients with sleep apnea: value of ultrafast MR imaging. AJR. *American journal of roentgenology*, 160(2), 311-314.

Thongdee, P., & Samman, N. (2005). Stability of maxillary surgical movement in unilateral cleft lip and palate with preceding alveolar bone grafting. *The Cleft palate-craniofacial journal,* 42(6), 664-674.

Tian, W., & Redett, R. J. (2009). New velopharyngeal measurements at rest and during speech: implications and applications. *Journal of Craniofacial Surgery*, 20(2), 532-539.

Tian, W., Yin, H., Li, Y., Zhao, S., Zheng, Q., & Shi, B. (2010). Magnetic resonance imaging assessment of velopharyngeal structures in Chinese children after primary palatal repair. *Journal of Craniofacial Surgery,* 21(2), 568-577.

Tindlund, R. S., Rygh, P., & Bøe, O. E. (1993). Orthopedic protraction of the upper jaw in cleft lip and palate patients during the deciduous and mixed dentition periods in comparison with normal growth and development. *The Cleft palate-craniofacial journal*, 30(2), 182-194.

Toms, A. P., Smith-Bateman, C., Malcolm, P. N., Cahir, J., & Graves, M. (2010). Optimization of metal artefact reduction (MAR) sequences for MRI of total hip prostheses. *Clinical radiology*, 65(6), 447-452.

Trindade, I. E., Yamashita, R. P., Suguimoto, R. M., Mazzottini, R., & Trindade Jr, A. S. (2003). Effects of orthognathic surgery on speech and breathing of subjects with cleft lip and palate: acoustic and aerodynamic assessment. *The Cleft palate-craniofacial journal*, 40(1), 54-64.

United States Federal Food and Drug Administration. (2021, February 18). Dental Amalgam Fillings. Retrieved November 11, 2022, from https://www.fda.gov/medical-devices/dental-devices/dental-amalgam-fillings.

Vallino, L. D., Zuker, R., & Napoli, J. A. (2008). A study of speech, language, hearing, and dentition in children with cleft lip only. *The Cleft palate-craniofacial journal*, 45(5), 485-494.

Vasant, M. R., Menon, S., & Kannan, S. (2009). Maxillary expansion in cleft lip and palate using quad helix and rapid palatal expansion screw. *Medical Journal Armed Forces India*, 65(2), 150-153.

Vikhoff, B., Ribbelin, S., Köhler, B., Ekholm, S., & Borrman, H. (1995). Artefacts caused by dental filling materials in MR imaging. *Acta Radiologica,* 36(3), 323-325.

Ward, E. C., McAuliffe, M., Holmes, S. K., Lynham, A., & Monsour, F. (2002). Impact of malocclusion and orthognathic reconstruction surgery on resonance and articulatory function: an examination of variability in five cases. *British Journal of Oral and Maxillofacial Surgery*, 40(5), 410-417.

Wassmund, M. (1927). Frakturen und luxationen des gesichtsschädels [Fractures and luxations of the facial skull].

Watts, G. D., Antonarakis, G. S., Forrest, C. R., Tompson, B. D., & Phillips, J. H. (2015). Is linear advancement related to relapse in unilateral cleft lip and palate orthognathic surgery?. *The Cleft Palate-Craniofacial Journal*, 52(6), 717-723.

Wein, B. B., Drobnitzky, M., Klajman, S., & Angerstein, W. (1991). Evaluation of functional positions of tongue and soft palate with MR imaging: initial clinical results. *Journal of Magnetic Resonance Imaging*, 1(3), 381-383.

Whaites, E., & Drage, N. (2013). Essentials of Dental Radiography and Radiology. Churchill Livingstone.

Willmar, K. (1974). On Le Fort I osteotomy; A follow-up study of 106 operated patients with maxillo-facial deformity. *Scandinavian journal of plastic and reconstructive surgery*, 12, suppl-12.

Wirthlin, J. O., & Shetye, P. R. (2013). Orthodontist's role in orthognathic surgery. *Seminars in plastic surgery*, 27(3), 137-144.

Wu, J. T., Huang, G. F., Huang, C. S., & Noordhoff, M. S. (1996). Nasopharyngoscopic evaluation and cephalometric analysis of velopharynx in normal and cleft palate patients. *Annals of plastic surgery*, 36(2), 117-22.

Yamaguchi, K., Lonic, D., & Lo, L. J. (2016). Complications following orthognathic surgery for patients with cleft lip/palate: a systematic review. *Journal of the Formosan Medical Association*, 115(4), 269-277.

Yang, S. (2019). What are the different parts of braces? [Web page]. Retrieved from https://orthodontistrwc.com/ortho-101/parts-of-braces/.

You, M., Li, X., Wang, H., Zhang, J., Wu, H., Liu, Y., ... & Zhu, Z. (2008). Morphological variety of the soft palate in normal individuals: a digital cephalometric study. *Dentomaxillofacial Radiology*, 37(6), 344-349.

APPENDIX A: Decision Tree for VP MRI in Patients with Orthodontic Appliances

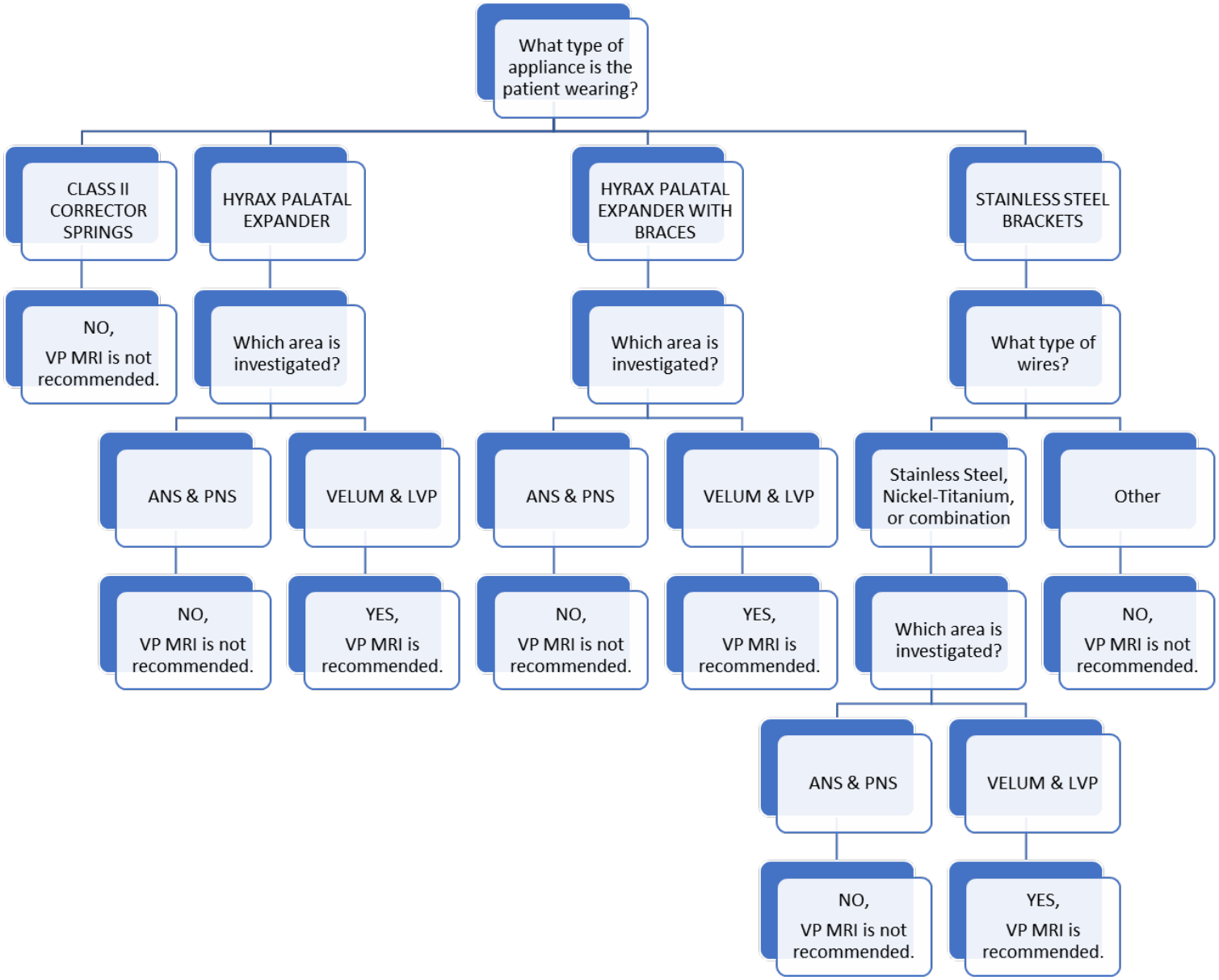

Appendix B: Guidebook for VP MRI in Patients with Orthodontic Appliances

A. Class II Corrector Springs
with stainless steel brackets and stainless steel wires and 4 molar bands

Location of molar bands:

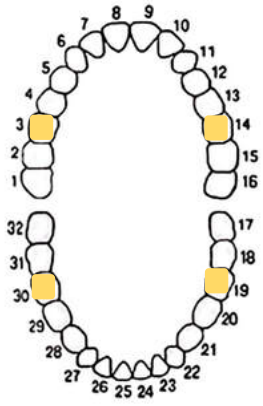

Oral Exam:

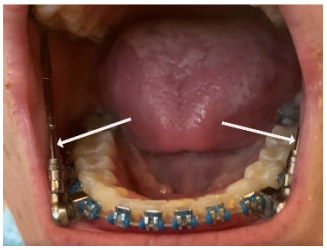

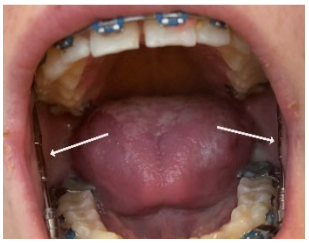

Appliance Details:

Brackets: 3M Unitek, Resilient Orthoform II Square stainless steel
Archwires: 19x25 stainless steel
Bands: 3M Victory Series Molar Bands, stainless steel
Class II Corrector Springs: PowerScope™ 2 Class II Corrector

MR images and MRI parameters:

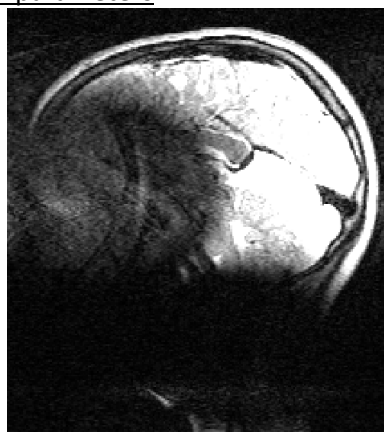

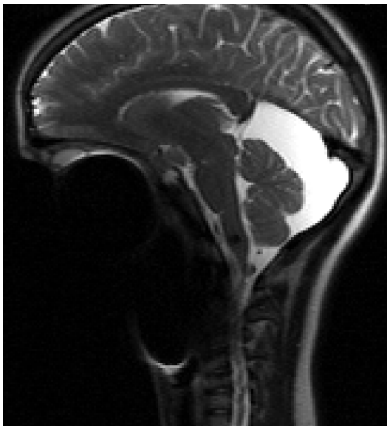

Sequence; Scan Name	HASTE; T2 SPACE	HASTE; 2D Mid-Sagittal	HASTE; 2D Oblique Coronal
TR; TE	2500ms; 265ms	1600ms; 119ms	1600ms; 119ms
Slice thickness	0.80mm	3.5mm	3.5mm
No. of Slices	192	4	4
Length of Scan	5 minutes, 7 seconds	7.9 seconds	7.9 seconds
Voxel Size	1.0 x 1.0 x 1.0mm	1.3 x 1.3 x 3.5mm	1.3 x 1.3 x 3.5mm

Velopharyngeal Variable Measures:

3D SPACE		2D Mid-Sagittal				2D Oblique Coronal	
Effective Velar Length	Sagittal Angle	Hard Palate Length	Velar Length	Pharyngeal Depth	Velar Knee to PPW	LVP muscle length	LVP Origin Distance
x	x	x	x	x	x	x	x

MRI Recommendation:

MRI of velopharyngeal mechanism is not recommended.

B. Hyrax Palatal Expander

Location of molar bands:

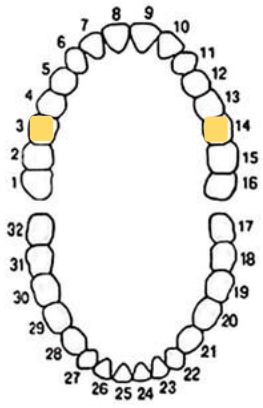

Oral Exam:

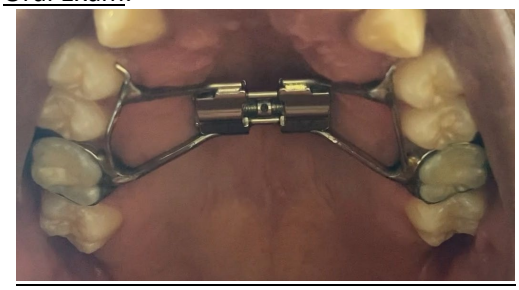

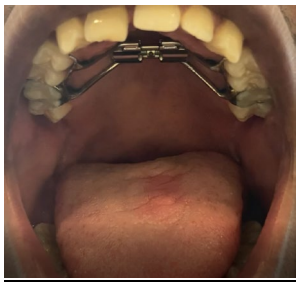

Appliance Details:

Bands: 3M Victory Series Molar Bands, stainless steel

Palatal Expander: Standard Rapid Palatal Expander by AccuTech Orthodontic Lab

MR images and MRI parameters:

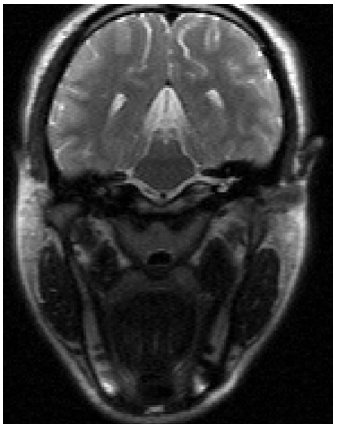

Sequence; Scan Name	HASTE; T2 SPACE	HASTE; 2D Mid-Sagittal	HASTE; 2D Oblique Coronal
TR; TE	2500ms; 265ms	1600ms; 119ms	1600ms; 119ms
Slice thickness	0.80mm	3.5mm	3.5mm
No. of Slices	192	4	4
Length of Scan	5 minutes, 7 seconds	7.9 seconds	7.9 seconds
Voxel Size	1.0 x 1.0 x 1.0mm	1.3 x 1.3 x 3.5mm	1.3 x 1.3 x 3.5mm

Velopharyngeal Variable Measures:

3D SPACE		2D Mid-Sagittal				2D Oblique Coronal	
Effective Velar Length	**Sagittal Angle**	**Hard Palate Length**	**Velar Length**	**Pharyngeal Depth**	**Velar Knee to PPW**	**LVP muscle length**	**LVP Origin Distance**
×	×	×	×	×	✓	✓	✓

MRI Recommendation:

MRI of velopharyngeal mechanism using two-dimensional HASTE sequence protocol at the mid-sagittal and oblique coronal plane is recommended.

B. Hyrax Palatal Expander
with stainless steel brackets with Nickel-Titanium wires (upper) & stainless steel wires (lower)

Location of molar bands:

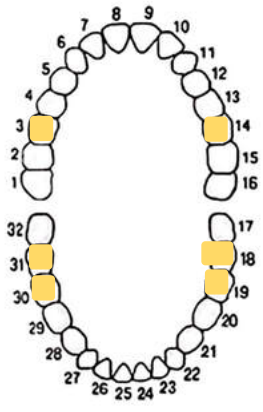

Oral Exam:

Appliance Details:
Brackets: Stainless Steel
Archwires: 018 NiTi Square; 17x25 SS Square
Bands: 3M Victory Series Molar Bands, stainless steel
Palatal Expander: Hyrax

MR images and MRI parameters:

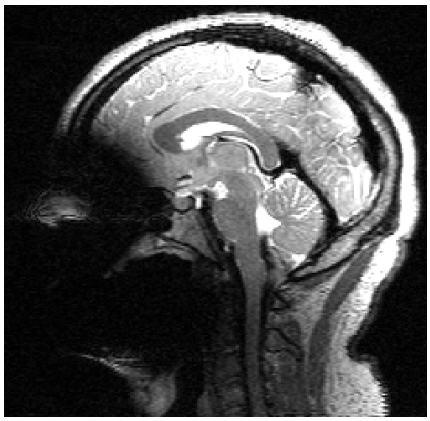

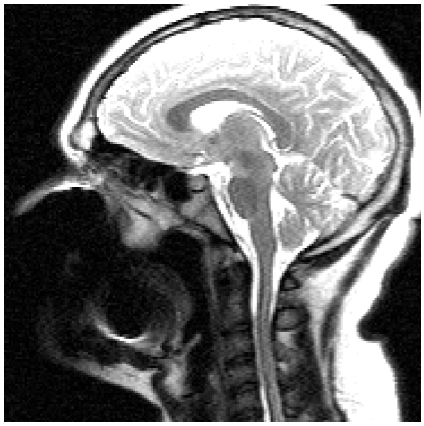

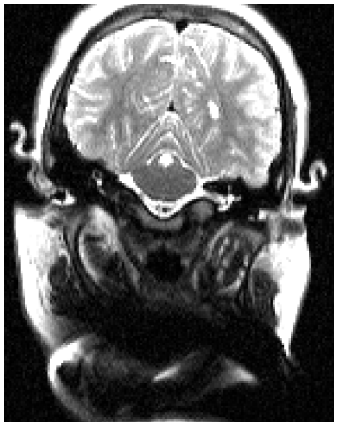

Sequence; Scan Name	HASTE; T2 SPACE	HASTE; 2D Mid-Sagittal	HASTE; 2D Oblique Coronal
TR; TE	2500ms; 265ms	1600ms; 119ms	1600ms; 119ms
Slice thickness	0.80mm	3.5mm	3.5mm
No. of Slices	192	4	4
Length of Scan	5 minutes, 7 seconds	7.9 seconds	7.9 seconds
Voxel Size	1.0 x 1.0 x 1.0mm	1.3 x 1.3 x 3.5mm	1.3 x 1.3 x 3.5mm

Velopharyngeal Variable Measures:

3D SPACE		2D Mid-Sagittal				2D Oblique Coronal	
Effective Velar Length	**Sagittal Angle**	**Hard Palate Length**	**Velar Length**	**Pharyngeal Depth**	**Velar Knee to PPW**	**LVP muscle length**	**LVP Origin Distance**
×	×	×	×	×	✓	✓	✓

MRI Recommendation:
MRI of velopharyngeal mechanism using two-dimensional HASTE sequence protocol at the mid-sagittal and oblique coronal plane is recommended.

C. Stainless Steel Brackets with Nickel-Titanium Wires

Location of molar bands:

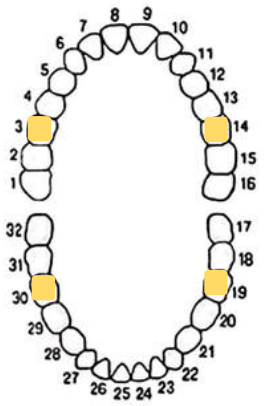

Oral Exam:

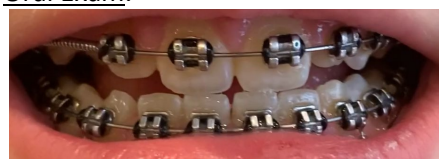

Appliance Details:

Bands: 3M Victory Series Molar Bands, stainless steel
Brackets: Stainless Steel
Archwires: 17x25 NiTi Square; 16x22 NiTi square; 19x25 NiTi Square; 014 NiTi Square; 016 NiTi Square; 018 NiTi Square; 17x25 NiTi Ovoid; 19x25 NiTi Ovoid
Other: Wire spring coil by Ortho Technology, stainless steel

MR images and MRI parameters:

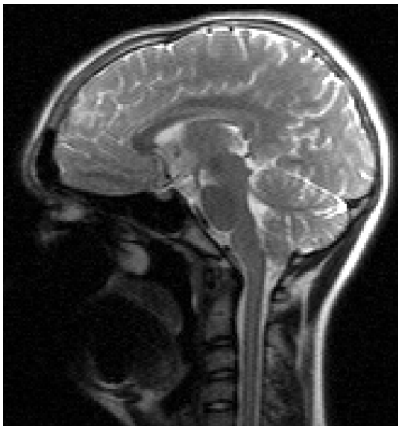

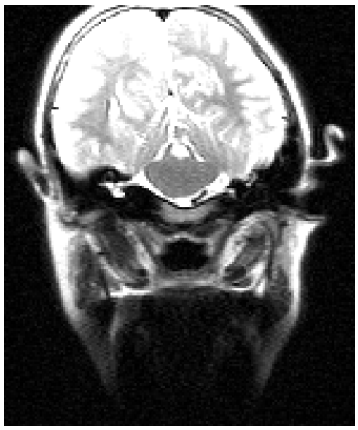

Sequence; Scan Name	HASTE; T2 SPACE	HASTE; 2D Mid-Sagittal	HASTE; 2D Oblique Coronal
TR; TE	2500ms; 265ms	1600ms; 119ms	1600ms; 119ms
Slice thickness	0.80mm	3.5mm	3.5mm
No. of Slices	192	4	4
Length of Scan	5 minutes, 7 seconds	7.9 seconds	7.9 seconds
Voxel Size	1.0 x 1.0 x 1.0mm	1.3 x 1.3 x 3.5mm	1.3 x 1.3 x 3.5mm

Velopharyngeal Variable Measures:

	3D SPACE		2D Mid-Sagittal				2D Oblique Coronal	
Number of Bands	Effective Velar Length	Sagittal Angle	Hard Palate Length	Velar Length	Pharyngeal Depth	Velar Knee to PPW	LVP muscle length	LVP Origin Distance
No bands	×	×	×	×	×	✓	✓	✓
One band	×	×	×	×	×	✓	✓	✓
Four bands	×	✓ [50%]	×	×	×	✓	✓	✓
Spring on wire	×	×	×	×	×	✓	✓	✓

MRI Recommendation:

MRI of velopharyngeal mechanism using two-dimensional HASTE sequence protocol at the mid-sagittal and oblique coronal plane is recommended.

D. Stainless Steel Brackets with Stainless Steel Wires

Location of molar bands:

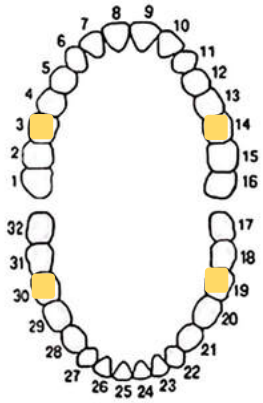

Oral Exam:

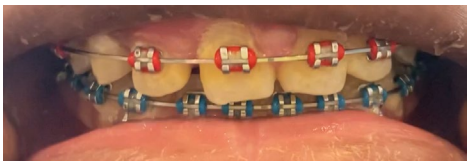

Appliance Details:

Brackets: Stainless Steel

Bands: 3M Victory Series Molar Bands, stainless steel

Archwires: 17x25 SS Ovoid, 19x25 SS Ovoid, 17x25 SS Square, 19x25 SS Square

MR images and MRI parameters:

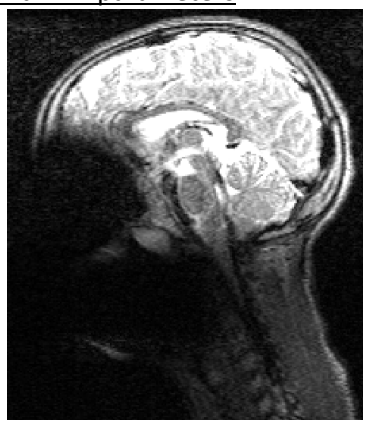

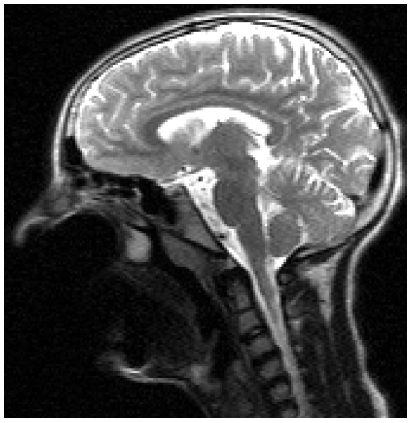

Sequence; Scan Name	HASTE; T2 SPACE	HASTE; 2D Mid-Sagittal	HASTE; 2D Oblique Coronal
TR; TE	2500ms; 265ms	1600ms; 119ms	1600ms; 119ms
Slice thickness	0.80mm	3.5mm	3.5mm
No. of Slices	192	4	4
Length of Scan	5 minutes, 7 seconds	7.9 seconds	7.9 seconds
Voxel Size	1.0 x 1.0 x 1.0mm	1.3 x 1.3 x 3.5mm	1.3 x 1.3 x 3.5mm

Velopharyngeal Variable Measures:

	3D SPACE		2D Mid-Sagittal				2D Oblique Coronal	
Number of Bands	Effective Velar Length	Sagittal Angle	Hard Palate Length	Velar Length	Pharyngeal Depth	Velar Knee to PPW	LVP muscle length	LVP Origin Distance
None	×	×	×	×	×	✓	✓	✓
Four	×	✓ [50%]	×	×	×	✓	✓	✓

MRI Recommendation:

MRI of velopharyngeal mechanism using two-dimensional HASTE sequence protocol at the mid-sagittal and oblique coronal plane is recommended.

E. Stainless Steel Brackets with Nickel-Titanium Wires (upper) & Stainless Steel wires (lower)

Location of molar bands:

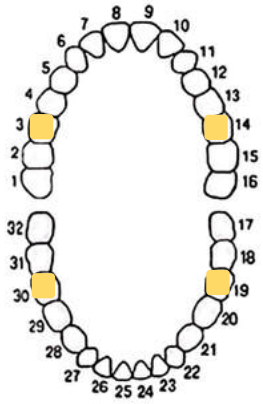

Oral Exam:

Appliance Details:

Bands: 3M Victory Series Molar Bands, stainless steel
Brackets: Stainless Steel
Archwires: 19x25 NiTi Ovoid; 19x25 SS Ovoid; 018 NiTi Square; 17x25 SS square
17x25 NiTi Ovoid; 17x25 SS Ovoid

MR images and MRI parameters:

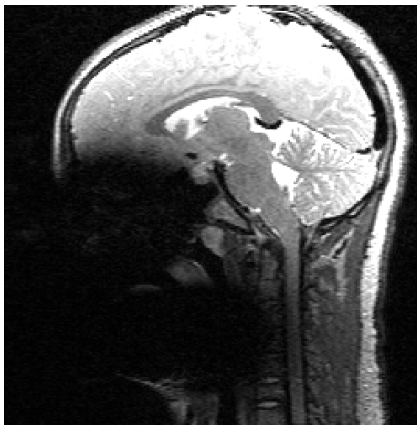

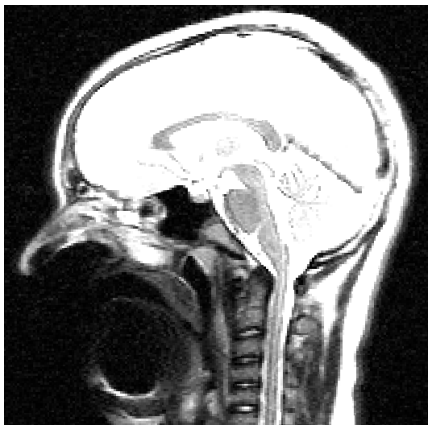

Sequence; Scan Name	HASTE; T2 SPACE	HASTE; 2D Mid-Sagittal	HASTE; 2D Oblique Coronal
TR; TE	2500ms; 265ms	1600ms; 119ms	1600ms; 119ms
Slice thickness	0.80mm	3.5mm	3.5mm
No. of Slices	192	4	4
Length of Scan	5 minutes, 7 seconds	7.9 seconds	7.9 seconds
Voxel Size	1.0 x 1.0 x 1.0mm	1.3 x 1.3 x 3.5mm	1.3 x 1.3 x 3.5mm

Velopharyngeal Variable Measures:

	3D SPACE		2D Mid-Sagittal				2D Oblique Coronal	
MRI Protocol	**Effective Velar Length**	**Sagittal Angle**	**Hard Palate Length**	**Velar Length**	**Pharyngeal Depth**	**Velar Knee to PPW**	**LVP muscle length**	**LVP Origin Distance**
No bands	×	×	×	×	×	✓	✓	✓
Two bands	×	×	×	×	×	✓	✓	✓
Four bands	×	✓	×	×	×	✓	✓	✓

MRI Recommendation:

MRI of velopharyngeal mechanism using two-dimensional HASTE sequence protocol at the mid-sagittal and oblique coronal plane is recommended.

APPENDIX C: Specifications of Orthodontic Appliances

Appliance Type/Part	**Trade Name**	**Company**	**Composition**
Class II corrector springs	Class II Correction Simplified	Power Scope 2	Stainless Steel
Hyrax palatal expander	Standard RPE	AccuTech Orthodontic Lab	Stainless Steel
Direct Bonding - Stainless Steel Brackets	Victory Series Low Profile Brackets	3M	Stainless Steel
Molar bands	3M Victory Series Molar Bands	3M	Stainless Steel
Stainless steel wires	17x25 SS Ovoid 19x25 SS Ovoid 17x25 SS Square 19x25 SS Square	3M Unitek Resilient Orthoform II	Stainless Steel
Nickel-Titanium wires	17x25 NiTi Square 16x22 NiTi square 19x25 NiTi Square 014 NiTi Square 016 NiTi Square 018 NiTi Square 17x25 NiTi Ovoid 19x25 NiTi Ovoid	Nitinol Heat-Activated OrthoForm III Ovoid	Nickel & Titanium
Wire Spring Coil	Closed Spring Coil 0.010”x0.030” Open Spring Coil 0.010”x0.030”	Ortho Technology	Stainless Steel

APPENDIX D: East Carolina University Institutional Review Board (IRB) Approval from 2021-2022

EAST CAROLINA UNIVERSITY
University & Medical Center Institutional Review Board
4N-64 Brody Medical Sciences Building· Mail Stop 682
600 Moye Boulevard · Greenville, NC 27834
Office **252-744-2914** · Fax **252-744-2284** ·
rede.ecu.edu/umcirb/

Notification of Continuing Review Approval: Expedited

From: Biomedical IRB
To: Jamie Perry
CC:
Jamie Perry
Jamie Perry
Date: 8/25/2021
Re: CR00009362
UMCIRB 11-001103
Variations in VP structure between upright and supine MRI in children and adults

The continuing review of your expedited study was approved. Approval of the study and any consent form(s) is for the period of 8/24/2021 to 8/23/2022. This research study is eligible for review under expedited category # 4,6. The Chairperson (or designee) deemed this study no more than minimal risk.

As the Principal Investigator you are explicitly responsible for the conduct of all aspects of this study and must adhere to all reporting requirements for the study. Your responsibilities include but are not limited to:

1. Ensuring changes to the approved research (including the UMCIRB approved consent document) are only initiated with UMCIRB review and approval except when necessary to eliminate an apparent immediate hazard to the participant. All changes (e.g. a change in procedure, number of participants, personnel, study locations, new recruitment materials, study instruments, etc.) must be prospectively reviewed and approved by the UMCIRB before they are implemented;

2. Ensuring that only valid versions of the UMCIRB approved, date-stamped informed consent document(s) are used for obtaining informed consent (consent documents with the IRB approval date stamp are found under the Documents tab in the ePIRATE study workspace);

3. Promptly reporting to the UMCIRB all unanticipated problems involving risks to participants and others;

4. Applying for continuing review and receive approval of continuation of the study prior to the study's current expiration date. Application for continuing review should be submitted no less than 30 days prior to the expiration date. Lapses in approval (i.e. study expiration) should be avoided to protect the safety and welfare of enrolled participants and liability to the University; and

5. Submission of a final report when the study meets the UMCIRB criteria for closure. Study approval should not be allowed to expire simply because the study is completed, rather the UMCIRB should be formally notified of study completion via the final report process.

The approval includes the following items:

Document	Description
Child Assent_Objective 1(0,07)	Consent Forms
Childrens Healthcare of Atlanta Flyer(0.03)	Recruitment Documents/Scripts
Coloring book for children(0,01)	Additional Items
data coding(0.01)	Data Collection Sheet
Dosher Recruitment Flyer(0,01)	Recruitment Documents/Scripts
FLYER (Clean copy).docx(0.01)	Recruitment Documents/Scripts
flyer-amendment 6 (clean copy)_updated 12-16-2020.docx(0,02)	Recruitment Documents/Scripts
HIPAA Authorization_adult_Updated 2-11-2021(0.01)	HIPAA Documentation
HIPAA Authorization_parent guardian_Updated 2-11-2021(0,01)	HIPAA Documentation
Informed Consent(adults)_Objective 2(0.15)	Consent Forms
Informed Consent(children)__Objective 1(0,15)	Consent Forms
letter for MRI (mail)_5_5_2018 (clean).docx(0.04)	Additional Items
letter for MRI (mail)_5_5_2018 (tracked).docx(0,07)	Additional Items
New Hanover Flyer (Clean copy)_updated 12-16-2020.docx(0.02)	Recruitment Documents/Scripts
Parental Consent_Objective 1(0,05)	Consent Forms
Phone script_Objectives (Clean copy)_updated 12-18-2020.docx(0.02)	Recruitment Documents/Scripts
Post-op Flyer_NHRMC (Clean copy)_updated 12-16-2020.docx(0,02)	Recruitment Documents/Scripts
Questionnaire_Objectives 1 and 2(0.03)	Surveys and Questionnaires
Samantha Power CITI Certification.pdf(0,01)	Recruitment Documents/Scripts
Script (email & phone) 5_5_2018 (clean).docx(0.02)	Additional Items
Script (email & phone) 5_5_2018 (tracked).docx(0,01)	Additional Items
Survey- Final yes no.docx(0,01)	Surveys and Questionnaires
The Research Protocol_1_13_20 tracked changes(0.16)	Study Protocol or Grant Application
The Research Protocol_1_13_20_clean copy(0.16)	Study Protocol or Grant Application

For research studies where a waiver or alteration of HIPAA Authorization has been approved, the IRB states that each of the waiver criteria in 45 CFR 164.512(i)(1)(i)(A) and (2)(i) through (v) have been met. Additionally, the elements of PHI to be collected as described in items 1 and 2 of the Application for Waiver of Authorization have been determined to be the minimal necessary for the specified research.

The Chairperson (or designee) does not have a potential for conflict of interest on this study.

IRB00000705 East Carolina U IRB #1 (Biomedical) IORG0000418
IRB00003781 East Carolina U IRB #2 (Behavioral/SS) IORG0000418

APPENDIX E: East Carolina University Institutional Review Board (IRB) Approval from 2022-2023

EAST CAROLINA UNIVERSITY
University & Medical Center Institutional Review Board
4N-64 Brody Medical Sciences Building· Mail Stop 682
600 Moye Boulevard · Greenville, NC 27834
Office **252-744-2914** · Fax **252-744-2284** ·
rede.ecu.edu/umcirb/

Notification of Continuing Review Approval: Expedited

From: Biomedical IRB
To: Jamie Perry
CC:
Jamie Perry
Jamie Perry
Date: 7/18/2022
Re: CR00009806
UMCIRB 11-001103
Variations in VP structure between upright and supine MRI in children and adults

The continuing review of your expedited study was approved. Approval of the study and any consent form(s) is for the period of 7/16/2022 to 7/15/2023. This research study is eligible for review under expedited category # 4, 6, 7. The Chairperson (or designee) deemed this study no more than minimal risk.

As the Principal Investigator you are explicitly responsible for the conduct of all aspects of this study and must adhere to all reporting requirements for the study. Your responsibilities include but are not limited to:

1. Ensuring changes to the approved research (including the UMCIRB approved consent document) are only initiated with UMCIRB review and approval except when necessary to eliminate an apparent immediate hazard to the participant. All changes (e.g. a change in procedure, number of participants, personnel, study locations, new recruitment materials, study instruments, etc.) must be prospectively reviewed and approved by the UMCIRB before they are implemented;

2. Ensuring that only valid versions of the UMCIRB approved, date-stamped informed consent document(s) are used for obtaining informed consent (consent documents with the IRB approval date stamp are found under the Documents tab in the ePIRATE study workspace);

3. Promptly reporting to the UMCIRB all unanticipated problems involving risks to participants and others;

4. Applying for continuing review and receive approval of continuation of the study prior to the study's current expiration date. Application for continuing review should be submitted no less than 30 days prior to the expiration date. Lapses in approval (i.e. study expiration) should be avoided to protect the safety and welfare of enrolled participants and liability to the University; and

5. Submission of a final report when the study meets the UMCIRB criteria for closure. Study approval should not be allowed to expire simply because the study is completed, rather the UMCIRB should be formally notified of study completion via the final report process.

The approval includes the following items:

Document	Description
Child Assent_Objective 1(0.07)	Consent Forms
Childrens Healthcare of Atlanta Flyer(0.03)	Recruitment Documents/Scripts
Coloring book for children(0.01)	Additional Items
data coding(0.01)	Data Collection Sheet
Dosher Recruitment Flyer(0.01)	Recruitment Documents/Scripts
FLYER (Clean copy).docx(0.01)	Recruitment Documents/Scripts
flyer-amendment 6 (clean copy)_updated 12-16-2020.docx(0.02)	Recruitment Documents/Scripts
HIPAA Authorization_adult_Updated 2-11-2021(0.01)	HIPAA Documentation
HIPAA Authorization_parent guardian_Updated 2-11-2021(0.01)	HIPAA Documentation
Informed Consent(adults)_Objective 2(0.15)	Consent Forms
Informed Consent(children)__Objective 1(0.15)	Consent Forms
letter for MRI (mail)_5_5_2018 (clean).docx(0.04)	Additional Items
letter for MRI (mail)_5_5_2018 (tracked).docx(0.07)	Additional Items
New Hanover Flyer (Clean copy)_updated 12-16-2020.docx(0.02)	Recruitment Documents/Scripts
Parental Consent_Objective 1(0.05)	Consent Forms
Phone script_Objectives (Clean copy)_updated 12-18-2020.docx(0.02)	Recruitment Documents/Scripts
Post-op Flyer_NHRMC (Clean copy)_updated 12-16-2020.docx(0.02)	Recruitment Documents/Scripts
Questionnaire_Objectives 1 and 2(0.03)	Surveys and Questionnaires
Samantha Power CITI Certification.pdf(0.01)	Recruitment Documents/Scripts
Script (email & phone) 5_5_2018 (clean).docx(0.02)	Additional Items
Script (email & phone) 5_5_2018 (tracked).docx(0.01)	Additional Items
Survey- Final yes no.docx(0.01)	Surveys and Questionnaires
The Research Protocol_1_13_20 tracked changes(0.16)	Study Protocol or Grant Application
The Research Protocol_1_13_20_clean copy(0.16)	Study Protocol or Grant Application

For research studies where a waiver or alteration of HIPAA Authorization has been approved, the IRB states that each of the waiver criteria in 45 CFR 164.512(i)(1)(i)(A) and (2)(i) through (v) have been met. Additionally, the elements of PHI to be collected as described in items 1 and 2 of the Application for Waiver of Authorization have been determined to be the minimal necessary for the specified research.

The Chairperson (or designee) does not have a potential for conflict of interest on this study.
